Recent developments in the study of parity violation in neutron *p* resonances

C. M. Frankle and S. J. Seestrom
Los Alamos National Laboratory, Los Alamos, NM 87545, USA

Yu. P. Popov and E. I. Sharapov
Joint Institute for Nuclear Research, 141980, Dubna, Russia

N. R. Roberson
Duke University, Durham, NC 27708, USA and Triangle Universities Nuclear Laboratory, Durham, NC 27708, USA

Fiz. Elem. Chastits At. Yadra **24**, 939–988 (July–August 1993)

Recent results in experimental and theoretical study of parity violation in neutron *p*-wave resonances are presented systematically. The emphasis is laid on the latest achievements at the LANSCE pulsed neutron source, where for the first time the weak matrix elements were obtained for several resonances in a single nucleus. An unexpected finding of the sign correlation among longitudinal asymmetries of the ^{232}Th neutron cross section is discussed. The established theoretical models and new approaches are reviewed in the framework of attempts to obtain information on the weak nucleon–nucleon interaction from parity-violating effects in compound nuclei.

1. INTRODUCTION

A new generation of experiments aimed at studying the weak interaction in nuclei, in order to resolve the problem of the weak nucleon–nucleon interaction, is reviewed in this article. The nonleptonic parity-violating (PV) interaction between hadrons is known to exist with the strength of

$$4\pi G m_\pi^2/g_{\pi NN}\approx 2\cdot 10^{-7} \tag{1}$$

relative to the parity-conserving (PC) interaction. Here m_π is the π-meson mass, G is the weak-interaction Fermi constant, and $g_{\pi NN}=13.45$ is the strong-interaction constant in the πNN vertex. There exist six weak meson–nucleon constants f_π^1, $h_\rho^{\Delta T}$, $h_\omega^{\Delta T}$ corresponding to the exchange of mesons with different changes ΔT of isospin. They are under active study in pp and $p\alpha$ scattering experiments.

The spin of the particle, $\boldsymbol{\sigma}$, is an important constituent in such experiments because it allows one to measure the amplitude F of the admixed state with parity $(-\pi)$ in the total wave function of the system

$$\psi=\psi^{(\pi)}+F\psi^{(-\pi)}. \tag{2}$$

The most productive class of experiments with effects in first order in F involves measurement of pseudoscalar observables of the $(\boldsymbol{\sigma}\cdot\mathbf{p})$ type (here $\mathbf{p}$ is the momentum of a particle) which are odd under parity inversion. This may be done in two ways: by producing (detecting) the longitudinal projection of a particle spin along its momentum, or by measuring the rotation around $\mathbf{p}$ of the particle spin which was initially oriented perpendicular to $\mathbf{p}$. Experiments with elementary particles, though straightforward in interpretation, suffer from small effects ($F\approx 10^{-7}$). Only broad ranges for the constants f_π and h_ρ have been obtained to date.

Since the experiment of Abov and co-workers[1] on the asymmetry of γ-quanta decay of cadmium after the capture of polarized thermal neutrons it is known that the PV effects in nuclei may be enhanced to the level of 10^{-4}. In the context of first-order perturbation theory for nuclear systems, the amplitude factor F_n is given by

$$F_n\equiv\alpha=\frac{\langle\pi^+|W|\pi^-\rangle}{E_{\pi^-}-E_{\pi^+}}\,d. \tag{3}$$

It is usually called the mixing coefficient and in such a case is denoted by α. The factor d here is a dynamical amplification factor. The single-particle weak potential W connected with the underlying nucleon–nucleon interactions was elaborated in the theory for describing the parity violation in nuclei. However, it was not widely used for heavy nuclei, owing to the lack of knowledge of the wave functions of complicated nuclear states resulting in the factor d. Besides, owing to interference of electric and magnetic multipoles in γ decay, another unknown factor, R, enters the asymmetry effect A_γ:

$$A_\gamma=\alpha R. \tag{4}$$

Only in light nuclei (e.g., as reviewed by Adelberger and Haxton[2]), where the nuclear wave functions and corresponding matrix elements were sufficiently reliable, was some quantitative information on the weak coupling constants obtained.

Beginning in 1981,[3] a series of measurements of the pseudoscalar term $(\boldsymbol{\sigma}\cdot\mathbf{p})$ in the total neutron cross section of low-energy p-wave resonances was carried out by Alfimenkov *et al.*[4] at the Dubna pulsed reactor. These experiments revealed PV effects as large as 10^{-2}–10^{-1}. An overview of these experiments, as well as the history of the early measurements with thermal neutrons, was given by Alfimenkov.[5] A polarized proton filter was used as a polarizer of resonance neutrons, and the longitudinal asymmetry

 1063-7796/93/040401-23$10.00

$$P=(\sigma_p^+-\sigma_p^-)/(\sigma_p^++\sigma_p^-) \quad (5)$$

in the total resonance cross section σ_p was measured for the resonances up to neutron energy $E_n \approx 20$ eV.

The asymmetry was analyzed using a model of compound nuclear-state mixing, and a simple expression was obtained from R-matrix theory:

$$P=\frac{2M}{(E_p-E_s)}\left(\frac{\Gamma_n^s}{\Gamma_n^p}\right)^{1/2}. \quad (6)$$

Here $M \equiv \langle s|V^{\mathrm{PV}}|p\rangle$ is the matrix element of the weak interaction between s and p compound states formed in the capture of s-wave (orbital angular momentum $l=0$) and p-wave ($l=1$) neutrons, $\Gamma_n^{s(p)}$ are the neutron widths of the s (p) resonances, and $E_{s(p)}$ are the corresponding resonance energies. The value obtained, $M \approx 1$ meV, agreed well with the expected statistical estimate $M_{\mathrm{theor}} = M_{\mathrm{SP}}/N^{1/2}$, where the value of the single-particle matrix element is $M_{\mathrm{SP}} \approx 0.5$ eV and $N \cong 10^6$ is the number of quasiparticle components in the wave function of a compound state.

The success of these experiments stimulated subsequent efforts by groups at LANL (Los Alamos), KEK (Tsukuba), and KIAE (Moscow). New setups for measurement of the $(\boldsymbol{\sigma}\cdot\mathbf{p})$ observable were created. Most of the Dubna results were repeated. The latest achievements have not been reviewed to date, and therefore in Sec. 2 we give an account of the technical accomplishments at LANSCE in producing and handling polarized beams of epithermal neutrons and in detecting very intense neutron fluxes.

In Sec. 3 we will proceed to the realm of the experimental results obtained for the helicity dependence of a neutron cross section near low-energy p-wave resonances. The latest Dubna–Gatchina results with thermal neutrons for the $^6\mathrm{Li}(n,\alpha)T$ and $^{35}\mathrm{Cl}(n,p)^{35}\mathrm{S}$ reactions will also be discussed, as they are directly connected with the problem under study. Using the advantage of the good time-of-flight resolution of their pulsed neutron source, the Los Alamos group has overcome the limitations of previous measurements and has studied parity violation for many resonances in a single nucleus. The statistically averaged mean-square matrix element

$$M^2=Av\{|\langle s|V^{\mathrm{PV}}|p\rangle|^2\} \quad (7)$$

was obtained for the first time.

The new experimental results on parity violation in neutron resonances triggered developments on the theoretical front aimed at obtaining information on weak coupling constants from a system in a chaotic regime where there is no detailed knowledge of the nuclear wave function. In particular, it was argued that M^2 depends mostly on the h_p^0 and f_π^1 constants. The other intriguing finding was the possible sign correlation of the P asymmetries for the thorium resonances, pointing to the possibility of some kind of collective effects which modify the statistical behavior of nuclei. All these topics will be covered in Sec. 4.

The study of parity-violation properties of the p-wave neutron resonances is now a rich and constantly growing field of research. In the concluding outlook of Sec. 5 we intend to give our ideas on what needs to be done in the near future to help to quantify the structure of the weak interaction by performing measurements of PV effects in nuclei.

2. EXPERIMENTAL FACILITIES

2.1. The LANSCE polarized neutron-beam facility

Polarized beams of slow neutrons have been extensively used for over 25 years in the experiments which test the fundamental symmetries of time-reversal invariance and parity conservation. A thorough survey of the methods of these experiments, including the methods of generating and analyzing polarized neutron beams, was given by Krupchitsky.[6] The technique for polarizing resonance neutrons by transmission through a polarized proton target was first developed and used at JINR, as reported in Ref. 7, and was followed by LANL[8] and KEK.[9,10] Owing to the nature of their facilities, both the JINR and KEK polarized-neutron spectrometers are limited in the maximum resonance energy that they can successfully reach. For JINR the limit is ≈ 20 eV, while for KEK it is ≈ 50 eV. As a result of this, neither facility has been able to measure more than one PV effect in any given nucleus.

The new generation of parity-violation experiments, which are being reviewed in this paper, are made possible by the availability of the intense epithermal neutron beam at the Los Alamos Neutron Scattering Center (LANSCE). It is generated by an 800-MeV proton beam from the Los Alamos Meson Facility (LAMPF) linac. This beam is injected into and accumulated by a proton storage ring (PSR). The injected beam consists of 600- to 800-μs wide macropulses with a repetition rate of 20 Hz. The macropulses are chopped at the low-energy end of the linac to produce a 110-ns gap every 360 ns.[11] Since the circulation time for 800-MeV protons in the PSR is 360 ns, the macropulse is wrapped around the PSR until the complete pulse is stored. The average target current at LANSCE is 60–70 μA. The accumulated contents of the PSR are extracted and transported to a tungsten production target, where the resulting spallation neutrons (about 17–18 per proton) are partially moderated by slabs of water and collimated to produce a beam of neutrons.[12] The spallation target and moderation system is located at the center of a cylindrical biological shield with outer radius 4.6 m. A more detailed discussion of the PSR can be found in Refs. 11, 13, and 14.

The available neutron flux has been measured with a small (1 cm thick and 1 cm in diameter) NE905 ^{6}Li-loaded glass scintillator. The neutrons were detected in the scintillator via the reaction

$$n+{}^6\mathrm{Li}\rightarrow{}^4\mathrm{He}+{}^3\mathrm{H}+4.78\ \mathrm{MeV}.$$

Since the cross sections for this reaction for epithermal neutrons can be expressed as $\sigma(\mathrm{barns}) = 149/\sqrt{E_n(\mathrm{eV})}$, the detection efficiency is known. With the detector located at a flight path of 56 m, the pulses resulting from the

neutron reaction in the scintillator were recorded with a multiscaler. The expression for the neutron intensity at the detector position has the form

$$\Delta N = K \frac{\Delta E_n}{(E_n)^\beta} i f t \Omega, \tag{8}$$

where ΔN is the number of neutrons with energies between E_n and $E_n + \Delta E_n$ per second; i is the average proton current in μA; f is the fraction of the moderator surface that the detector views through the beam line collimators (the total surface is 13 cm$\times$13 cm; $f=0.11$ for these measurements); t is the attenuation factor due to air and absorptive materials in the beam; Ω is the detector solid angle in sr ($\Omega \cong S/R^2$, where S is the detector area and R is the distance from the moderator); and β and K are constants. A least-squares fit of Eq. (8) to the ^{6}Li-detector data gave the parameters $\beta=0.9$ and $K=3.5 \cdot 10^{10}$ (sr $\cdot \mu$A $\cdot$ sec)$^{-1}$.

The overall energy resolution of the neutron beam is determined primarily by the proton-beam burst width, the time spread from the moderator, and the detector thickness. The proton beam has an approximate shape of an isosceles triangle with a base width of 250 ns and a standard deviation of 51 ns. The time-spread FWHM introduced by the moderator has been calculated by Michaudon and Wender[13] and varies from about 6600 ns (1 eV) to 200 ns (1000 eV). For a 1-cm thick detector located at 56 m the energy resolution $\Delta E_n/E_n$ is nearly constant and equal to $3 \cdot 10^{-3}$ up to 1000 eV.

The neutron beam is polarized by transmission through a sample containing polarized protons. Since the n–p spin–spin cross section is large and approximately constant over a wide energy range ($\sim$1 eV to 50 keV), a polarized proton target makes an ideal epithermal-neutron spin filter. This technique was implemented for the first time at Dubna in the work of Ref. 7. The refurbished target used at LANSCE was originally built by Keyworth *et al.*[8] The protons, located in the water of hydration of single crystals of $La_2(0.05\%\ Nd)Mg_3(NO_3)_{12} \cdot 24H_2O$, abbreviated as LMN, are polarized with microwaves using the so-called solid-state effect.[15,16] This is a mature technology, so only the most salient features are discussed here.

Six flat LMN crystals, forming a block 3.5$\times$3.5 cm^2 by 1.8 cm thick, are inside a microwave cavity and immersed in a pumped 1.2 K liquid-helium bath. The crystals are in a 2T magnetic field, produced by a superconducting magnet, the field of which is oriented along the beam direction. At liquid-helium temperatures the magnetic properties of Nd^{3+} can be described by an effective-spin $S=1/2$ Hamiltonian. The lowest energy levels are determined by the orientation of "electron"–proton pairs. By applying microwave power at 75.520 or 75.685 GHz one of two possible forbidden transitions occurs in which the "electron" and proton spins are flipped together. Since the electron spin-lattice relaxation time is much shorter than the proton spin-lattice relaxation time, the proton system becomes polarized. The proton polarization for this system has been typically 37–38%; the resulting neutron polarization was about 40%. The transmission through the spin filter is energy-dependent but is about 13% from 1 eV to 100 eV. For a typical beam line such as the one at LANSCE (see Fig. 2.1), the flux is further decreased by about a factor of 2 by windows in the spin filter, end caps on the vacuum pipes, and several meters of air. Therefore, the polarized-neutron flux is, for the range from 1 eV to 100 eV, approximately 6–7% of the unpolarized flux.

Fast-neutron spin reversal is accomplished by passing the beam through a spatially varying system of magnetic fields. This device is called the "spin flipper" and consists of a pair of longitudinal solenoids and a pair of transverse coils; a schematic view is shown in Fig. 2.2. The solenoids are configured to produce longitudinal fields of the same magnitude but with opposite directions (Fig. 2.2). In one configuration the transverse field is off, and the total field is produced by the longitudinal solenoids alone. A neutron entering the flipper along the z axis and with spin parallel to the z axis will experience no torque, since $\mathbf{r}=\boldsymbol{\mu}\times\mathbf{B}=0$, where $\boldsymbol{\mu}$ is the neutron magnetic moment. Therefore, to first order, all neutrons will pass through the spin flipper with the spin directions unchanged, as shown in Fig. 2.2.

In the second configuration, the transverse field is on, producing a component B_x, which is plotted in the lower part of Fig. 2.2. The transverse field can be either parallel or antiparallel to the x axis. If the Larmor frequency of the neutron in the total magnetic field is large relative to the magnetic-field rotation experienced by a neutron with velocity v, the neutron spin adiabatically follows the direction of the total magnetic field. For a neutron entering the spin flipper with spin parallel to the beam direction ($+z$ direction), the spin direction will rotate clockwise or counterclockwise, depending on the direction of B_x, and will exit the spin flipper with spin reversed. Bowman and Tippens[17] have studied the spin behavior for neutron trajectories which are close to but not on the z axis. Figure 2.3 shows, as a function of the neutron energy, the spin-flipper efficiencies for a total magnetic field of 100 G and a circular beam of radius $R=1.4$ cm. The efficiencies plotted in Fig. 2.3 are the average of the spin-preserving efficiency ($B_x=0$) and the spin-flip efficiency ($B_x \neq 0$).

The polarization of the neutron beam is related to the magnitude of the proton polarization of the spin filter by

$$f_n = \tanh(f_p n \sigma_p t), \tag{9}$$

where n is the proton-number density, t is the crystal thickness, and f_p is the proton polarization. The quantity σ_p is the spin-dependent part of the total cross section given by

$$\sigma^{\pm} = \sigma_0 \mp \sigma_p f_n, \tag{10}$$

where $\sigma_0=20.5$ b, $\sigma_p=16.7$ b,[7] and $\sigma^{+(-)}$ is the cross section for neutron spins parallel (antiparallel) to the polarized protons. The transmission of the neutron beam through the crystal is given by

$$T = e^{-\alpha} e^{-n\sigma_0 t} \cosh(f_p n \sigma_p t), \tag{11}$$

where $e^{-\alpha}$ represents the spin-independent absorption by nuclei other than protons.

The neutron-beam polarization f_n can be derived from the LMN proton polarization, using Eq. (9). The proton polarization of the sample can be measured by the nuclear-

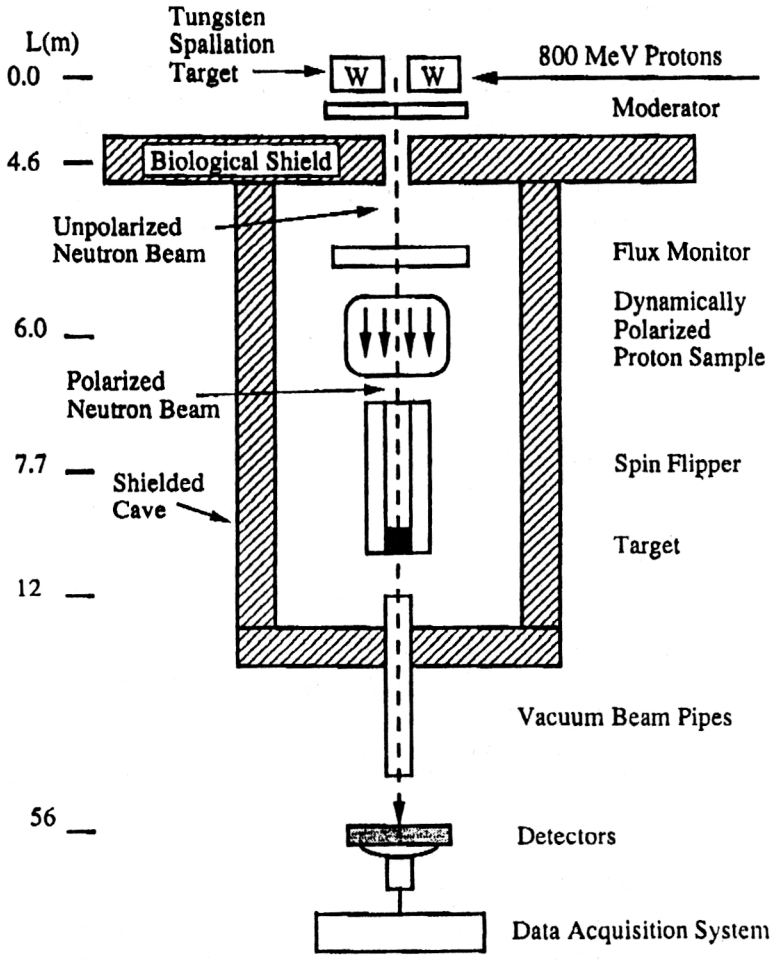

FIG. 2.1. Schematics of the beam line as used for tests of parity violation at LANSCE.

magnetic-resonance (NMR) technique. It is possible that f_p is overestimated or underestimated for some geometries and sample material, owing to the fact that the NMR coil does not measure the sample equally or that the sample material is not homogeneous. Nonuniform proton polarization can result from imperfections within the crystals, temperature gradients, gaps, radiation damage, or other problems. A second method for determining f_p is to measure the transmission of the neutrons through the spin-filter sample and use Eq. (11) to extract f_p. If the polarization of the spin-filter sample is nonuniform across the transmitted beam, then the subsequent value of f_n will be incorrect. A discussion of how these problems affect the accuracy of transmission measurements of f_n was given by Yuan *et al.*[18]

There exists a method which can be used to establish the neutron polarization absolutely, independently of the detailed condition of the spin-filter crystals. The method involves measuring the parity-violating longitudinal analyzing power P of the 0.734-eV p-wave resonance in ^{139}La. The experimental technique for measuring P is the subject of this review and will be discussed in more detail in Sec. 2.2. Briefly, one measures the transmission asymmetry [see Eq. (10)] for the 0.734-eV ^{139}La resonance and determines the quantity f_nP. The value of P, the parity-violating longitudinal analyzing power, has been measured to be $(9.55 \pm 0.35)\%$, using a double-target arrangement[18] which does not require an independent knowledge of the polarization. By using the known value of P, the polarization of the neutron beam, f_n, is determined. An NMR signal can be recorded simultaneously and used subsequently to monitor the neutron polarization.

The sequence in which the neutron spins are flipped during a measurement can be selected to minimize systematic errors. The spin flipper, as discussed above, was designed so that the current through the transverse coil can be reversed and the neutron spins can be flipped by rotating the spin either clockwise or counterclockwise. An eight-step sequence 0, +, −, 0, +, 0, 0, −, where 0 represents the period when the transverse field is off, and + (−) represents the period when the transverse field is on and is either $\pm B_x$, cancels, in first order, the effects on the detector photomultiplier tubes of stray magnetic fields from the transverse coil and cancels linear and quadratic time drifts in the detectors.[19]

The neutrons were detected with a system of ^{6}Li-loaded glass detectors located at 56 m from the neutron source. Owing to the very high count rates involved, the detectors were operated in the current mode.[20] The neutron beam was monitored with a ^{3}He ionization chamber placed directly in front of the spin flipper. After each eight-step sequence the average neutron flux is determined and the data are accepted only if the average flux is within a predetermined range (normally $\pm 8\%$). Each step in the

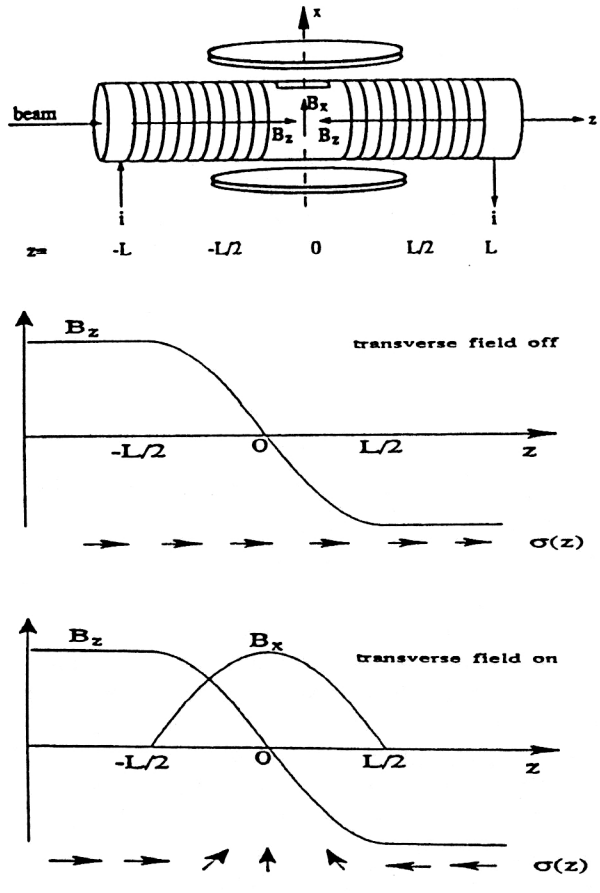

FIG. 2.2. Spin-flipper schematics. The axial magnetic field with the transverse field equal to zero and the spin orientation of the transmitted neutrons are shown in the center.

eight-step sequence lasted 200 neutron bursts (10 s). The sequence was then repeated 20 times, and this collection of data (20 eight-step sequences) was combined into a "run." These runs were then treated as the basic unit of data.

2.2. Measurement techniques

There are two primary techniques for measuring parity violation in neutron resonances. The first is via neutron transmission through a thick target ($n\sigma \approx 2$); the other is by measuring the total neutron-capture cross section with a thin target ($n\sigma \ll 1$). The transmission method measures the total neutron cross section, which has the form

$$\sigma_{\text{tot}} = \frac{\pi}{k^2} \frac{g_J \Gamma_n \Gamma}{(E-E_p)^2 + (\Gamma/2)^2}, \tag{12}$$

which is of course a Breit–Wigner shape for a single isolated resonance. Typically, for a p-wave resonance $\Gamma = \Gamma_n + \Sigma_i \Gamma_{\gamma i} = \Gamma_n + \Gamma_\gamma \approx \Gamma_\gamma$, where the sum is over all possible gamma decays from the state in question. Hence, if one observes all the gamma rays from a decaying resonance, which yields a cross section of the form

$$\sigma_\gamma = \frac{\pi}{k^2} \frac{g_J \Gamma_n \Gamma_\gamma}{(E-E_p)^2 + (\Gamma/2)^2}, \tag{13}$$

the same information is obtained as in a transmission experiment. Therefore, in principle transmission and total-capture experiments are identical for the purposes of studying parity violation. In practice both have certain experimental difficulties that at times make one preferable over the other.

2.2.1. Transmission

The basic technique for a neutron-transmission experiment is to send a well collimated neutron beam through a target and observe (detect) the neutrons that remain in the beam after the beam passes through the target. The detector must be placed sufficiently far away from the target, so such that only neutrons which are traveling in the strictly forward direction are detected. This distance is typically tens to hundreds of meters, depending on the geometry of the experiment and on the resolution required. One must also be cautious with the collimation geometry, as neutrons

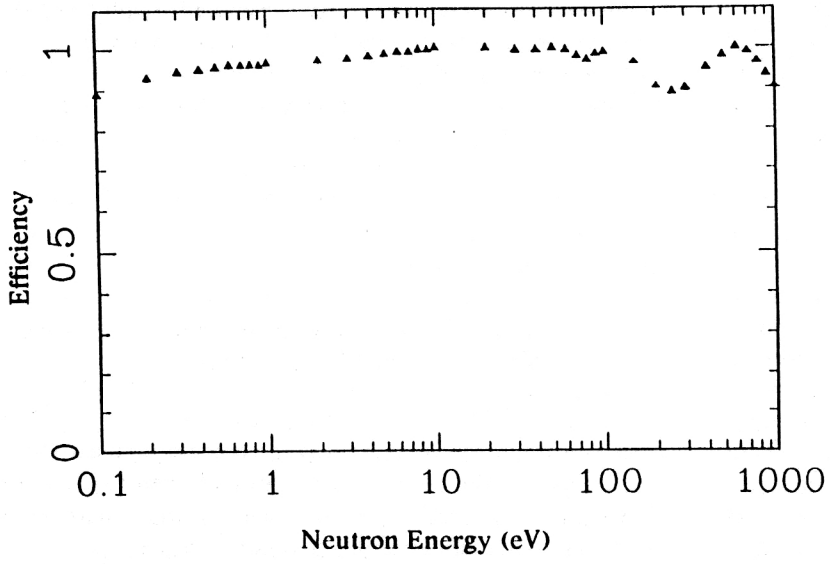

FIG. 2.3. The spin-flipper efficiencies versus the neutron energy for $B_v = 100$ G. The efficiency is defined in the text.

which are detected but did not have an opportunity to interact in the target, or interacted in some other material in or near the beamline, will alter the observed transmission. The major disadvantage of transmission experiments to study parity violation is that since one is interested in p-wave resonances which have $\sigma_p \sim 1$ b, target thicknesses of the order of 10 cm are required to achieve the optimal error conditions, $n\sigma = 2$. If one has a beam of several cm in diameter, then material quantities of the order of kg are required for targets. This is not practical for most isotopes which may be interesting to study.

Several different neutron detection techniques have been utilized in the study of parity violation. In general, neutron detection techniques have been well reviewed (e.g., Harvey and Hill[21]), so only details of interest will be discussed here.

At JINR a sectioned 210-l liquid-scintillator detector has been used at 54 m. Six sections are placed in a ring geometry about the beam to cover 90% of the 4π solid angle. The bore is 30 cm and the outer diameter is 73 cm. This is essentially a gamma detector. It was used as a neutron detector with the aid of a neutron–gamma converter made of 1.23 kg of Eu_2O_3, 1.3 kg of Tb_2O_3 and 1 l of H_2O. The high multiplicity of gamma cascades in such absorbers allowed the efficient use of twofold coincidences with a level of discrimination of about 0.5 MeV. The neutron efficiency of this detector changes from 40% to 30% for neutron energies from 1 eV to 500 eV. Besides this detector, several measurements at shorter distances were made with a standard 1-cm thick, 12.7-cm diameter ^{6}Li-glass scintillator.

The KEK transmission experiment on ^{139}La utilized a standard commercial ^{10}B-loaded liquid scintillator (NE311A).[22] This scintillator has 5% ^{10}B loading. In the past, the TRIPLE collaboration experiments at LANSCE have utilized ^{6}Li-glass scintillators (NE905). The detector was in the form of 12.7-cm diameter, 1-cm thick disks of Li-glass attached to 12.7-cm photomultiplier tubes. Seven such individual detectors were put together to form an array of 38.1 cm in diameter. A new detector using ^{10}B-loaded liquid is being developed but with a higher (8%) ^{10}B concentration to improve timing characteristics. This detector has 55 cells of 5.1 cm in diameter, 4-cm thick, each backed by a 5.1-cm photomultiplier tube. The overall detector has a diameter of 38.1 cm.

2.2.2. Total capture

A neutron total-capture experiment is conceptually simple. A target, usually a thin disk of material, is placed in a collimated neutron beam of approximately the same diameter as the target. A gamma-ray detector of near-4π solid angle is placed around the beam and target, though not usually in the beam. Some difficulties are introduced in implementing this for a parity-violation experiment, as the neutron polarization must be preserved all the way up to the target. This usually involves a system of magnetic fields which may necessitate additional forms of magnetic shielding for the detector photomultiplier tubes. An additional difficulty in capture experiments is multiple-scattering corrections when the target is not thin. This is introduced in the analysis of the data and can be overcome, though extraction of asymmetries is less straightforward than in the case of transmission.

Like transmission experiments, a variety of techniques have been used for the detection of gamma rays. As before, this field has been well reviewed (e.g., Knoll[23]), and only details specific to various parity-violation experiments will be discussed.

The KEK detector for neutron total-capture measurements uses BaF_2 crystals. The crystals are formed in a ring geometry about the beam. Approximately 85% of the 4π solid angle is covered. The total thickness of crystal in the gamma emission direction was 6 cm. Since BaF_2 is sensitive to scattered neutrons, a B_4C neutron shield is imposed between the target and the crystals. A discriminator is then set to reject events with less than 1 MeV gamma-ray energy. The exterior of the detector is shielded with B_4C, boric acid resin, and lead. At LANSCE a gamma-ray detector is under development. It has not yet been used for parity-violation experiments. It will utilize a ring geometry of CsI (pure) crystals. The crystals will be 10-cm thick in the gamma emission direction, resulting in an effective solid angle (actual solid angle times detection efficiency) of 66% of 4π. Like BaF_2 CsI (pure) is sensitive to scattered neutrons. The detector will be shielded from the target with 10% ^{6}Li-loaded polyethylene. The exterior of the detector will be shielded with boron-loaded polyethylene and lead.

3. EXPERIMENTAL RESULTS

3.1. Analysis of transmission data

We will first detail the techniques for extracting from measurements the PV asymmetries P defined by Eq. (5). The neutron total cross section is given by

$$\sigma = \sigma_{\text{pot}} + \sigma_p(1 \pm P), \tag{14}$$

where σ_{pot} is the potential-scattering cross section, σ_p is the resonance cross section, and P is the parity-violating asymmetry. Here it has been assumed that the only spin dependence occurs in the resonance cross section. The neutron transmission T through a target of n atoms per barn is defined in terms of the total cross section as

$$T = e^{-n\sigma}. \tag{15}$$

A transmission asymmetry ε can be defined as

$$\varepsilon = \frac{N^+ - N^-}{N^+ + N^-} = -\tanh(n\sigma_p f_n P), \tag{16}$$

where $N^{\pm}$ are the detector counts in the $\pm$ helicity states. This expression can be approximated by

$$\varepsilon \approx -n\sigma_p f_n P, \tag{17}$$

when the argument of the hyperbolic tangent is small. One could simply take the observed value of ε and obtain a value for P. This would, however, ignore many experimental effects which influence the observed cross section. Con-

sequently, it is best to fit simultaneously both spin states to a line shape which takes into account various experimental effects.

In principle, one may fit the spectra to extract the experimental resonance cross section for the two spin states $\sigma^{\pm}_{\rm exp}$. If the polarization f_n were 100%, these experimental cross sections could be substituted into Eq. (5) to calculate the asymmetry P. However, f_n is always less than 100%, and one writes

$$P=\frac{1}{f_n}\frac{\sigma^{+}_{\rm exp}-\sigma^{-}_{\rm exp}}{\sigma^{+}_{\rm exp}+\sigma^{-}_{\rm exp}}. \tag{18}$$

In the case of a well isolated resonance, fitting can be accomplished by use of a code which incorporates a single Breit–Wigner resonance shape with suitable experimental effects included. This approach has been successfully implemented for all but one of the resonances studied to date. As an example, the technique used by the TRIPLE collaboration at LANSCE will be described.

The code used by the TRIPLE collaboration fits data of two helicity states simultaneously. The data are fitted to a function of the form

$$Y^{\pm}=\frac{N(1\pm\beta)}{k-k_0}\left[1+\sum_{i=1}^{5}\alpha_i z^i\right]\exp[-n\phi(C)\sigma(B,\sigma_0) \times(1\pm f_n P)]. \tag{19}$$

Fits are done on a detector yield function Y which may represent either actual neutrons (counting mode) or digitized photomultiplier-tube current (current mode). In Eq. (19), N is the normalization constant, k is the time-of-flight channel number, k_0 is the resonance peak channel, and β is a normalization adjustment to the different helicity states where more neutrons may have been counted in one state than in the other. The α_i are parameters used to model the beam flux and detector efficiency, while the variable z is given by

$$z=\frac{k-(k_3+k_4)/2}{1000}, \tag{20}$$

where k_3 and k_4 are the lowest and highest channel numbers of a window set to include the resonance. The function ϕ is responsible for all types of Gaussian broadening of the resonance. It represents the sum of Gaussians due to Doppler broadening, broadening due to finite time resolution, plus any other broadening components which are Gaussian in nature. The function ϕ depends on the energy and on a width scaling parameter C. The Breit–Wigner single-level cross section is a function of the parameters B and σ_0, where B scales the natural width and σ_0 scales the peak cross section. The combination f_nP is the neutron polarization times the parity-violating asymmetry. All the parameters may be varied, though in practice most are determined by a fit to a set of summed data.

The data are fitted on a run-by-run basis for each resonance, where each run lasts one half hour of live beam time. In this way a value of P_{ij} is obtained for each resonance i and run j. The final value P_i for each resonance is then a weighted average of the P_{ij} values obtained from several hundred runs. The weighting factors are the errors assigned to the values of f_nP by the fitting code. Errors on P_i can be analyzed in several ways. In the case where the fitted data were actual neutron counts as opposed to digitized current, the error on P_i may be obtained from the errors given by the fitting code. Additionally, an error can be obtained by computing the standard deviation of the mean of the several hundred values of P_{ij} available for each resonance. This is a very robust method of calculating errors and is typically the value quoted. This technique does, however, assume that the errors are Gaussian.

The bootstrap method[24] can also be applied to a distribution of P values in order to test for the presence of non-Gaussian errors. Typically, 10 000 samples are generated for each distribution of P's to determine the bootstrap distribution. The bootstrap distribution is then examined for evidence of non-Gaussian character, and the central 68% of the distribution is computed and compared with the standard deviation of the mean.

As more and more resonances are studied it is inevitable that cases will be encountered where two or more resonances lie sufficiently close together that use of a single-level code is inappropriate. This has so far occurred only in the case of the 128.2-eV p-wave and 129.2-eV s-wave resonances in ^{232}Th. In such a case a multilevel code is required. For the previously mentioned case in ^{232}Th the code SAMMY[25] was used. Since the code SAMMY was described in great detail by Larson,[25] details will not be given here.

3.2. Analysis of capture data

In most respects the analysis of capture data is very similar to the analysis of transmission data. In the case of a thin sample, the following expression is valid for the capture asymmetry ε_γ:

$$\varepsilon_\gamma\equiv\frac{N^{+}_{\gamma}-N^{-}_{\gamma}}{N^{+}_{\gamma}+N^{-}_{\gamma}}=f_nP. \tag{21}$$

The major difference between the two types of measurements is the need to include multiple-scattering corrections in the extraction of P values from capture data. In the case of any finite-thickness target there is some probability that a neutron will elastically scatter before being captured by a nucleus. Once the neutron has scattered nearly all its polarization, information is lost. Hence as the thickness of the target increases the observed value of P will decrease. At the present time the normal method of correcting for multiple scattering is by numerical simulation.

Capture measurements can have a sensitivity advantage over transmission because there is no contribution from potential scattering. Any actual gain will depend on the neutron intensity on the sample and on the background level in the capture experiment. Capture is favored for thin targets, especially for isotopic samples, large quantities of which will be impossible to obtain. It is particularly advantageous for weak resonances.

TABLE III.1. Compilation of the measured parity-violating asymmetries in the mass-100 region.

Nucleus	Measurement	E_p (eV)	$g\Gamma_n$ (meV)	P (%)	Reference
^{81}Br	σ_{tot}	0.88	0.000058	2.4±0.4	[4,29]
	σ_γ			2.1±0.2	[26]
	σ_{tot}			1.77±0.33	[27]
^{111}Cd	σ_{tot}	4.53	0.00107	−0.86±0.12	[4, 30]
	σ_γ			$-1.3^{+0.7}_{-0.4}$	[26]
^{113}Cd	σ_γ	7.0	0.00031	−0.98±0.30	[31]
^{117}Sn	σ_{tot}	1.33	0.00019	0.45±0.13	[4, 29]
	σ_{tot}			0.77±0.13	[32]
	σ_γ			1.1±0.2	[33]
^{139}La	σ_{tot}	0.73	0.000036	7.3±0.5	[4, 29]
	σ_{tot}			7.6±0.6	[32]
	σ_{tot}			9.7±0.5	[22]
	σ_γ			9.5±0.3	[22]
	σ_{tot}			9.2±1.7	[34]
	σ_{tot}[(a)]			9.55±0.35	[18]
	σ_{tot}			10.15±0.45	[18]

[(a)]Polarization-independent experiment using two La targets.

3.3. Summary of experimental results

Since the first measurements of parity violation in neutron resonances began approximately a decade ago a total of 16 resonances have shown parity violation in seven different nuclei. We review all the successful experimental results to date. Relevant experimental details of each measurement will be given. Each nucleus will be discussed separately, and each measurement for a particular nucleus will be discussed if there were more than one. Only in two of the seven nuclei, multiple effects have been observed and both measurements have come from LANSCE, where the procedure of extraction of M^2 from the experimental data was implemented for the first time.

3.3.1. ^{81}Br

Bromine is not a particularly well studied nucleus. Until the discovery by Alfimenkov *et al.*[4] of the 0.88-eV resonance in ^{81}Br there were no known p-wave levels in either stable bromine isotope. The assignment of the 0.88-eV resonance to ^{81}Br was the result of the study of the gamma-decay scheme of ^{82}Br. Despite being studied at two other laboratories besides JINR, there are still no other known p-wave resonances.

The 0.88-eV resonance has been studied for the purpose of investigating parity violation three times,[4,26,27] once each at JINR, KEK, and LANSCE. The first measurement was published by Alfimenkov *et al.*[4] as a result of work performed at JINR using the IBR-30 pulsed reactor. For the bromine measurement the reactor was operated with a neutron pulse width of 70 μs and a mean power level of 20 kW. Data were taken in the transmission mode, and the detector was located at the end of a 58-m flight path. Detectors of either liquid scintillator or Li glass were used. The total measurement time was approximately 250 h. Polarized neutrons were provided by use of a dynamically polarized proton filter. The filter material was LMN. Neutron polarizations were typically 50–60%. The polarization direction of the polarized proton target was reversed every 50 h. The neutron spin was reversed every 40 s. The thickness of ^{81}Br in the target was 0.11 at/b.

The 0.88-eV ^{81}Br resonance has been measured at KEK. Results of this measurement have been published by Shimizu.[26] During the bromine measurement there was an average of 3 μA of 500-MeV protons on the uranium spallation target. The proton burst width was 40 ns FWHM. An annulus of BaF_2 gamma-ray detectors was used to measure the asymmetry in the neutron total capture cross section. The detector was located 7 m from the neutron source. The target was CBr_4. The neutron beam was polarized by using a dynamically polarized proton filter with the proton polarization in the vertical direction. The polarizing filter material was ethylene glycol. Typical neutron polarizations were 70%. The neutron spins were rotated from the vertical to the direction along the beam axis by use of slowly changing magnetic guide fields. The direction of neutron spin was reversed every 4 s.

The parity-violating asymmetry in the 0.88-eV resonance of ^{81}Br has also been measured at LANSCE. This measurement has been published by Frankle *et al.*[27] While the bromine measurement was under way, the typical LANSCE beam current was 50 μA of 800-MeV protons on a tungsten spallation target. The proton burst width was 270 ns. A target of natural liquid bromine was used. The liquid was contained in a 10-cm diameter glass vessel with vessel axis of symmetry oriented perpendicular to the beam axis. An array of seven ^{6}Li glass detectors was used to measure the neutron transmission through the bromine target. The detector array was located at the end of a 56-m flight path. The total measurement time was approximately 45 h. Polarized neutrons were provided by use of a dynamically polarized proton filter. The filter material was LMN. Neutron polarizations were typically 45%. The polarization direction of the polarized proton target was reversed once per day of live time. Fast spin reversal was accom-

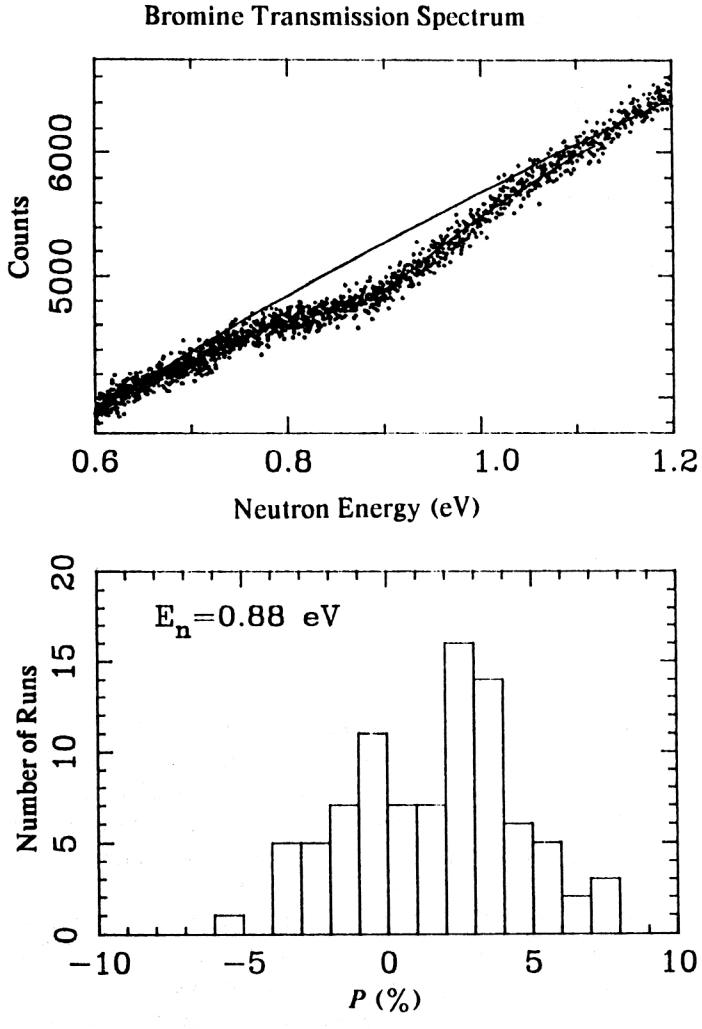

FIG. 3.1. Upper part: Sample fit of the 0.88-eV ^{81}Br resonance. Data are for one spin state of a half-hour LANSCE run. The top curve is the nonresonant portion of the fit, while the bottom curve is the full fit. Lower part: Histogram of the 89 values of P obtained from the 89 LANSCE data runs.

plished by means of a magnetic spin rotator (spin flipper). Spins were reversed in an eight-step sequence designed to minimize systematic errors. The neutron spin was reversed every 10 s.

Results of the three measurements are listed in Table III.1. All three measurements are consistent in both magnitude and sign. The weighed average of the three values is $2.14\pm0.16\%$. A sample spectrum from one of the spin states of a half-hour LANSCE run is shown in Fig. 3.1 (upper). Figure 3.1 (lower) is the histogram of the values of P from each of the 89 half-hour LANSCE runs used in the analysis of the LANSCE data.

3.3.2. ^{111}Cd

There are several known p-wave resonances in ^{111}Cd. The last comprehensive study of the resonance region of ^{111}Cd was by Liou *et al.*[28] The first p-wave resonance observed by Liou *et al.* was at 114.8 eV. Subsequently, Alfimenkov *et al.*[4] observed two other p-wave resonances at 4.53 and 6.94 eV.

The mass-111 isotope of cadmium has been studied for parity violation, twice at JINR and once at KEK.[4,30,26] Both measurements yielded consistent nonzero results for the 4.53-eV resonance. The 6.94-eV resonance was measured only at JINR and showed no significant parity violation, as expected, since the spin J for this resonance is $J=0$ according to gamma-ray measurements of the JINR group reported by Sharapov.[35] The measurement technique used at KEK was identical to that described in the section on ^{81}Br. The beam parameters at JINR were essentially the same as for the bromine measurement, but the reactor was operated with a 4-μs pulse width and an average power level of 5 kW. A portion of the JINR transmission spectrum is shown in Fig. 3.2 (upper) along with the transmission asymmetry (lower). The weighted average for the two measurements for the 4.53-eV resonance is $-0.90\pm0.10\%$. The results of the individual measurements are listed in Table III.1.

3.3.3. ^{113}Cd

The two p-wave resonances in ^{113}Cd with energies 7.0 eV and 21.9 eV were first reported by the JINR group.[31] Measurements with much better resolution were made at LANL by Frankle *et al.*;[36] altogether 22 new resonances were observed in the neutron energy region 20–500 eV. The values of the resonance energies and neutron widths were obtained. The resonances were assumed to be p-wave on the basis arguments of their very weak neutron widths.

This isotope is of particular interest for the study of parity violation because it was in ^{113}Cd where Abov *et al.*[1]

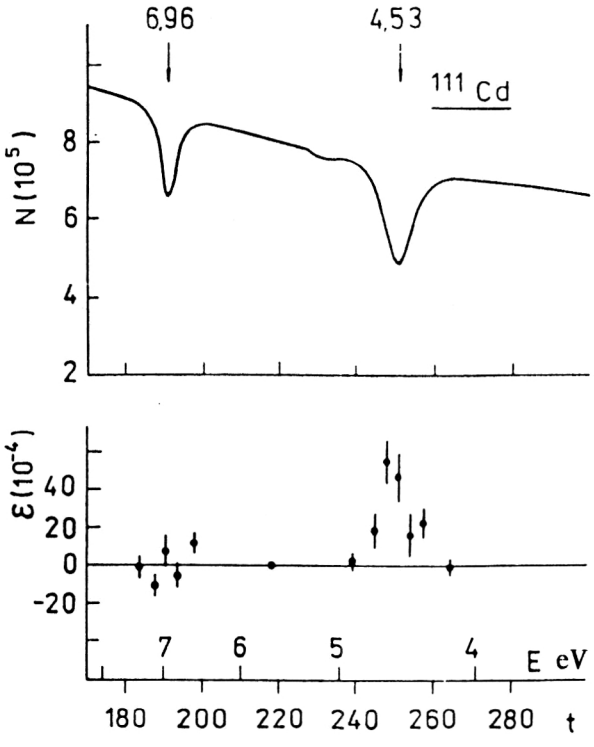

FIG. 3.2. Upper part: A portion of the JINR transmission spectrum for ^{111}Cd. Lower part: The observed transmission asymmetry from the JINR data.

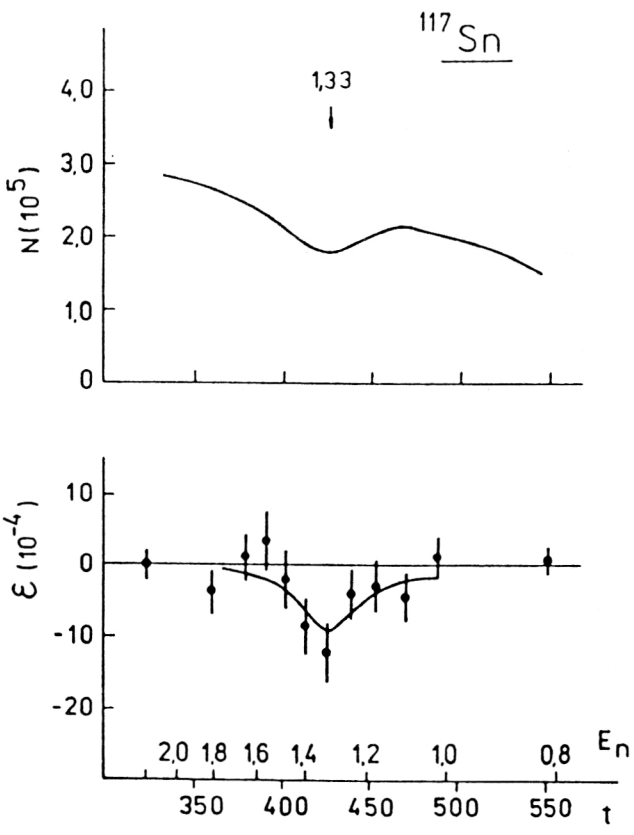

FIG. 3.3. Upper part: A portion of the JINR transmission spectrum for ^{117}Sn. Lower part: The observed transmission asymmetry from the JINR data.

first discovered an enhancement of parity violation in nuclei in an experiment with thermal neutrons. Transmission measurements of longitudinal asymmetries in the resonance region were conducted at JINR with the use of their modernized setup. Namely, the old proton polarized target was moved closer to the neutron source (9 m instead of the previous 30 m) and the new highly efficient ^{3}He detector (multisectioned proportional ionization chamber) was installed at 30 m and put into operation. The intensity of the polarized neutron beam just behind the polarizer was equal to $3 \cdot 10^5 E^{-0.9}$ n/eV · sec, where E is in eV. The parameters of the pulsed neutron source were the same as for the ^{111}Cd measurements. The result obtained for the 7.0-eV resonance is $-(0.98 \pm 0.30)\%$ and is the only one for ^{113}Cd at this time.

3.3.4. ^{117}Sn

There is one known p-wave resonance in ^{117}Sn. This resonance has an energy of 1.33-eV. The last comprehensive study of this nucleus was more than 20 years ago. The only recent data on resonances in ^{117}Sn was reported by Sharapov *et al.*[33] They observed a new weak resonance at 26.4 eV. No parameters were assigned.

Parity violation for the 1.33 eV resonance in ^{117}Sn has been measured three times. The three measurements were performed at JINR, IAE and LANSCE.[4,32,33] Results of the three measurements are listed in Table III.1. In sign the three measurements agree, but in magnitude their errors do not overlap. The weighted average of the three is $0.70 \pm 0.08\%$.

The first measurement of parity violation in the 1.33-eV resonance of ^{117}Sn was performed by Alfimenkov *et al.*[4,29] The experimental procedure for the measurement was identical to that given in the section on ^{81}Br. The principal isotope thickness of the target was 0.13 at/b. A portion of the JINR transmission spectrum is shown in Fig. 3.3 (upper) along with the transmission asymmetry (lower).

The 1.33-eV resonance was studied at the Kurchatov Institute of Atomic Energy. Results were reported by Biryukov *et al.*.[32] The measurement was performed with the KIAE linear electron accelerator. The accelerator was operated with 10 kW of beam power dissipated in the uranium neutron-production target. Pulse repetition rates were varied between 550 and 700 Hz with pulse widths between 100 and 300 ns. The experiment was performed in a polarizer–analyzer configuration with the neutrons first passing through the ^{117}Sn target, then a spin flipper, and finally a polarized-proton filter acting as the analyzer. The polarized-proton filter used ethylene glycol as the filter material. The proton polarization was typically 45% for the ^{117}Sn measurement. The neutron spin was reversed every 15 s. Neutrons were detected by a transmission-type detector located 12 m from the neutron source.

The final measurement of the 1.33-eV resonance in

^{117}Sn performed to date was done at LANSCE. The results of this measurement were reported by Sharapov *et al.*[33] Details of the measurement were generally similar to that of the ^{81}Br measurement, but with a few exceptions. The tin sample was 92% enriched in the mass-117 isotope and was fabricated into a target with thickness 0.029 at/b. The target was located 22.5 m from the neutron source. The experiment looked at gamma rays from neutron capture in the target. Gamma rays were detected by a pair of $15\times15\times15$-cm BaF_2 crystals located 10 cm from the beam center on either side of the target. Discriminators were set so that only gamma rays with energy between 1 and 5 MeV were counted. Typical neutron polarizations for this experiment were 17%.

3.3.5. ^{139}La

The nucleus ^{139}La is unique in several ways. Until recently the parity-violating effect on the 0.73-eV resonance was the largest known. Secondly, it is by far the most studied nucleus of all those in which parity violation has been observed. Finally, even though it was the largest effect reported, conflicting values have been given for the asymmetry. Results of all the measurements are summarized in Table III.1.

The first reported measurement of parity violation in the 0.73-eV resonance of ^{139}La was by Alfimenkov *et al.*[4,29] The experimental procedures for this experiment are identical to those reported for the bromine measurement. The measured value of the parity violation was $7.3\pm0.5\%$. The transmission spectrum and transmission asymmetry for this measurement are shown in Fig. 3.4 (upper and lower, respectively). This measurement was repeated several years later at KIAE by Biryukov *et al.*.[32] The value $7.6\pm0.6\%$ obtained by Biryukov *et al.* was consistent with that obtained at JINR. Procedures used by Biryukov *et al.* were identical to those described in the section on ^{117}Sn.

Two measurements were performed at KEK, both reported by Masuda *et al.*.[22] One result was obtained by measuring the total neutron-capture cross section. Techniques for this measurement were identical to those described in the section on bromine. The value $9.5\pm0.3\%$ was obtained, in clear conflict with the two values obtained at JINR and at KIAE. The parity-violating asymmetry was also measured by neutron transmission. For that experiment a ^{10}B-loaded liquid scintillator (NE311A) detector was placed 9.4 m from the neutron source. The incident-beam intensity was monitored with a uranuim fission chamber placed at 4 m. A value $9.7\pm0.5\%$ was obtained in the transmission experiment. An early experiment at LANSCE attempted to resolve the discrepancy between the JINR/KIAE results and the KEK results. This experiment was reported by Bowman *et al.*[34] Polarization was provided by a laser-pumped ^{3}He cryostat, and the neutron transmission was measured at a flight path of 11 m with a ^{6}Li glass detector. The result $9.2\pm1.7\%$ was obtained.

Since that time the Dubna group repeated the measurements, with the result[31] $9.5\pm0.5\%$, and two additional experiments have been performed at LANSCE. Both were reported by Yuan *et al.*[18] The first measurement was similar to that described in the section on bromine. Typical neutron polarizations were 43%. The beam pulse repetition rate was 15 Hz for this measurement. The target consisted of 0.065 at/b La in the form of La_2O_3 powder. The total running time was slightly less than 24 h. The value obtained for the parity-violating asymmetry was $10.15\pm0.45\%$. A second experiment was performed later, with a very different experimental arrangement. Instead of a polarized-proton filter to provide polarized neutrons, a lanthanum metal target was used to give the neutron beam a slight polarization due to the parity violation in the 0.73-eV resonance. A second La metal target was then used as an analyzer, and the results were interpreted in a way independent of the beam polarization. All other components of the system remained the same, including the spin flipper and detector array. The two targets were identical disks of La metal, 5.080 cm in diameter and 5.105 cm thick. The two targets were placed at opposite ends of the spin flipper so that their separation was 2 m. The total running time was about 40 h. The measured asymmetry from the double lanthanum experiment was $9.55\pm0.35\%$. This is considered to be the most reliable of all lanthanum experiments.

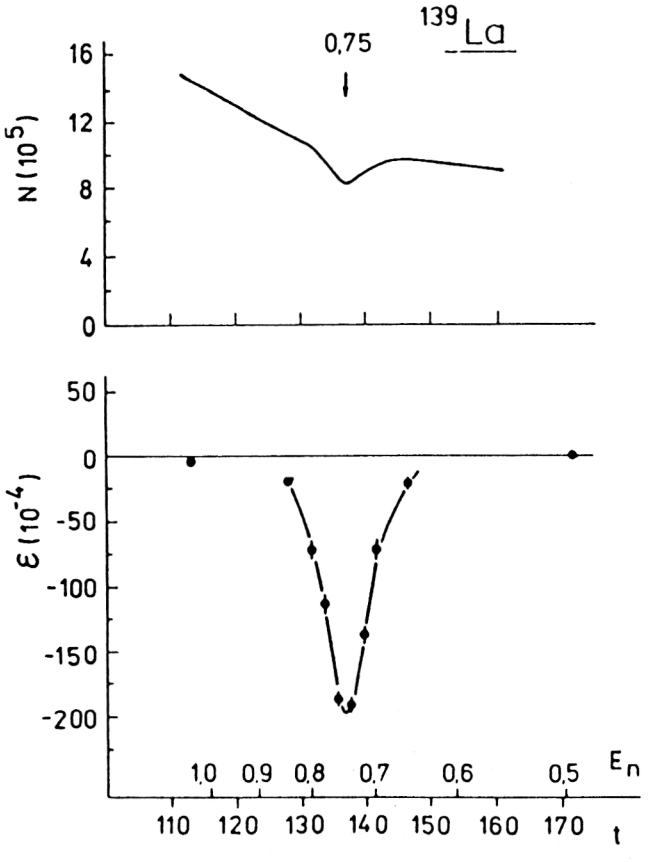

FIG. 3.4. Upper part: A portion of the JINR transmission spectrum for ^{139}La. Lower part: The observed transmission asymmetry from the JINR data.

3.3.6. ^{232}Th

The nucleus ^{232}Th has spin zero and an *s*-wave resonance level spacing of 16.4 eV in the latest evaluation.[37]

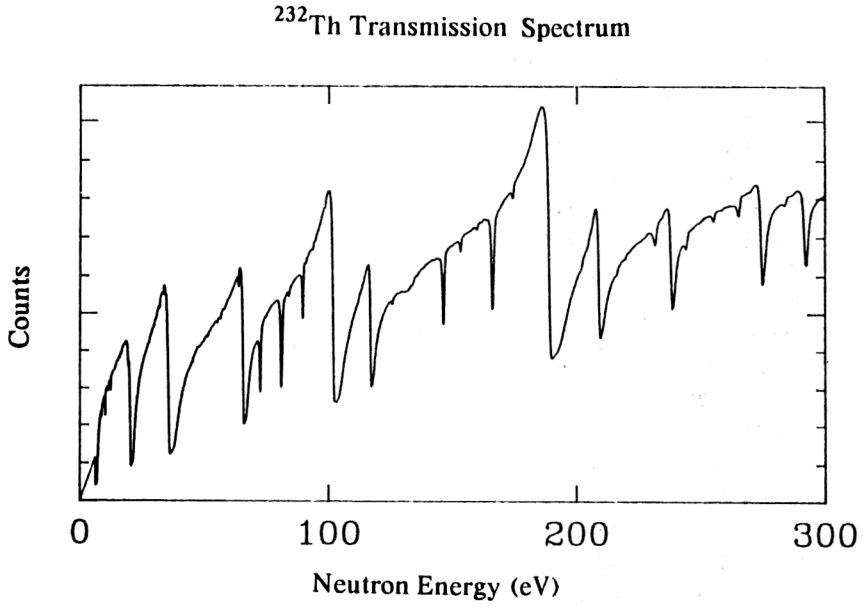

FIG. 3.5. A ^{232}Th transmission spectrum up to 300 eV from LANSCE.

The combination of zero spin and a fairly high level density makes this nucleus an attractive candidate for the study of parity violation. Olsen[37] lists 39 p-wave resonances in the region 0–400 eV. Of this set 23 have been studied for parity violation, with the 8.3-eV resonance having been studied at both JINR[38] and LANSCE[39,40] and the remainder only at LANSCE.

The JINR experiment was substantially similar to the one previously described for ^{111}Cd. The result 1.79 $\pm$0.92% was obtained for the 8.3-eV resonance.

A substantial effort has been made by the TRIPLE collaboration at LANSCE to measure parity violation in multiple resonances in a given nucleus at neutron energies up to several hundred eV. The nucleus ^{232}Th was the second one reported by the TRIPLE collaboration, the first one being ^{238}U, discussed in the next subsection. For the thorium experiment the average LANSCE beam current was about 60 μA at a repetition rate of 20 Hz and a burst width of 250 ns. The neutron-beam flux was monitored by using a ^{3}He-filled ionization chamber located just downstream from the neutron polarizer. Neutrons were detected by using an array of seven ^{6}Li glass scintillators operated in the "current mode" described in Sec. 2. Typical neutron polarizations for the experiment were 27%. The target was thorium metal, with a thickness of 0.093 at/b. The target was cooled to liquid-nitrogen temperature in order to reduce Doppler broadening of the resonances. A total of 185 hours of data were taken, though seven hours of data were later removed from the data set when it was discovered that the target had been inadvertently allowed to warm. A spectrum of the summed data is shown in Fig. 3.5. Of the 39 p-wave resonances listed in the Olsen evaluation, three were not observed and, for reasons discussed by Frankle *et al.*,[40] were assumed to be not in ^{232}Th. Of the remainder, 13 were not analyzed, either because of insufficient resolution or because they lay too close to a contaminant resonance. Hence a group of 23 resonances were analyzed; the results are given in Table III.2 and are displayed graphically in Fig. 3.6. Of the 23 resonances analyzed, seven showed parity-violation effects differing from zero by more than 2.4 standard deviations. The standard deviation was obtained by calculating the standard deviation of the mean of the 355 values of P obtained for each resonance, one from each of the 355 half-hour data runs used in the analysis. The largest of the effects, 10.9$\pm$2.3% on the 38.2-eV resonance, is the largest seen to data in any resonance, and the value 9.8$\pm$2.1% on the 64.5-eV resonance is nearly as large. This data set also contains the highest-energy effect yet observed, 1.10$\pm$0.46% on the 196.2-eV resonance. One interesting phenomenon observed in this data set is that all effects with statistical significance greater than 2-sigma are positive. This raises the possibility of the existence of correlations in the sign of the asymmetries, the details and implications of which will be discussed in Sec. 4.

3.3.7. ^{238}U

Because of its unique place in the field of nuclear physics, uranium has the distinction of being one of the most well studied nuclei from the nuclear-data standpoint. Both the Japanese Nuclear Data Committee and the U.S. National Nuclear Data Center have recently issued new evaluations for ^{238}U.[43,44] The new evaluations have substantially changed the ^{238}U level scheme from the older evaluations; however, none of the resonances which have been studied for parity violation have had their angular-momentum assignments changed.

There have been only two experiments performed on ^{238}U to look for parity violation. Alfimenkov *et al.*[4] studied the 4.4-, 11.3-, and 19.5-eV resonances. No significant parity violations were observed. The TRIPLE collaboration has also studied ^{238}U at LANSCE. An analysis of 17 resonances was reported by Bowman *et al.*[41] A subsequent reanalysis dropped the 57.9-eV resonance because of contamination by nearby ^{235}U resonances.[42] The results of all measurements on ^{238}U are listed in Table III.3.

The LANSCE measurement on ^{238}U was performed on a room-temperature target of depleted uranium (0.2%

TABLE III.2. Parity-violating asymmetries for the p-wave resonances in ^{232}Th.

E_p (eV)	Measurement	$g\Gamma_n$ (meV)	P (%)	Reference
8.3	σ_{tot}	0.000275	1.79±0.92	[38]
			1.48±0.25	[39, 40]
13.1	σ_{tot}	0.0002095	0.74±0.62	[39, 40]
37.0	σ_{tot}	0.0009407	2.5±1.0	[39, 40]
38.2	σ_{tot}	0.0005758	10.9±2.3	[39, 40]
41.0	σ_{tot}	0.0005868	−2.2±2.1	[39, 40]
49.9	σ_{tot}	0.0004833	−1.1±3.0	[39, 40]
64.5	σ_{tot}	0.0006940	9.8±2.1	[39, 40]
90.2	σ_{tot}	0.006145	−1.05±1.00	[39, 40]
98.1	σ_{tot}	0.003976	−0.01±1.38	[39, 40]
103.7	σ_{tot}	0.00554	−0.43±1.04	[39, 40]
128.2	σ_{tot}	0.06857	1.31±0.18	[39, 40]
145.9	σ_{tot}	0.08919	−0.03±0.22	[39, 40]
148.1	σ_{tot}	0.01035	−4.9±2.8	[39, 40]
167.2	σ_{tot}	0.01865	3.5±1.2	[39, 40]
179.0	σ_{tot}	0.0294	−1.47±1.28	[39, 40]
196.2	σ_{tot}	0.08172	1.10±0.46	[39, 40]
202.7	σ_{tot}	0.0305	2.2±1.4	[39, 40]
211.0	σ_{tot}	0.01629	1.76±1.85	[39, 40]
242.3	σ_{tot}	0.04192	−0.1±1.2	[39, 40]
299.8	σ_{tot}	0.04152	−1.6±1.7	[39, 40]
302.7	σ_{tot}	0.1415	−1.8±1.0	[39, 40]
380.7	σ_{tot}	0.1229	1.1±1.8	[39, 40]
391.8	σ_{tot}	0.1445	−0.7±1.6	[39, 40]

^{235}U). The target thickness was 0.12 at/b. Neutron beam intensities were monitored with a 1-mm thick ^{6}Li glass scintillator paddle inserted into the beam just upstream of the polarized proton filter. Typical LANSCE proton-beam currents were 50 μA. The neutron polarization was typically 45%. The total measurement time was just over 90 h. A sample spectrum is shown in Fig. 3.7. The data were taken using 8192 time-of-flight channels, each with width 200 ns. In practice this allowed analysis of the data from 6 eV to 300 eV. Of the 16 resonances included in the final analysis, four showed parity-violating effects at a level greater than two standard deviations. Standard deviations were calculated in the same manner as for the ^{232}Th data. Of the four nonzero asymmetries, two are positive and two are negative. The asymmetries are shown as a function of the resonance energy in Fig. 3.8.

3.3.8. ^{6}Li and ^{35}Cl

At first sight these light nuclei appear to be out of place in the review, as the measurements were performed with

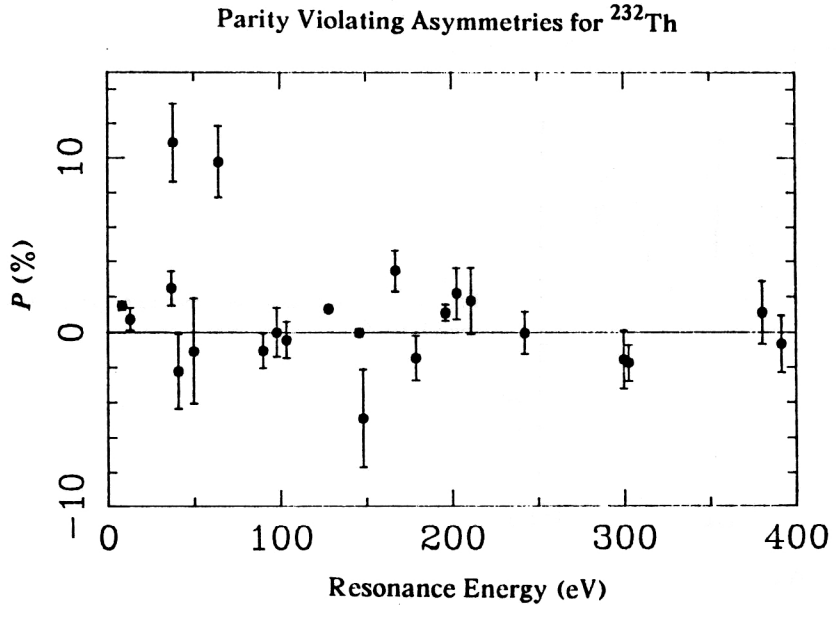

FIG. 3.6. The parity-violating asymmetries for 23 resonances in ^{232}Th.

TABLE III.3. Parity-violating asymmetries for the p-wave resonances in ^{238}U.

E_p (eV)	Measurement	$g\Gamma_n$ (meV)	P (%)	Reference
4.4	σ_{tot}	0.00011	0.37±0.37	[4]
10.2	σ_{tot}	0.00165	−0.16±0.08	[41, 42]
11.3	σ_{tot}	0.00039	0.25±0.25	[4]
			0.67±0.37	[41, 42]
19.5	σ_{tot}	0.0013	0.00±0.10	[4]
45.2	σ_{tot}	0.00090	−1.31±2.10	[41, 42]
63.5	σ_{tot}	0.0058	2.63±0.40	[41, 42]
83.7	σ_{tot}	0.0069	1.96±0.86	[41, 42]
89.2	σ_{tot}	0.085	−0.24±0.11	[41, 42]
93.1	σ_{tot}	0.006	−0.03±2.30	[41, 42]
98.0	σ_{tot}	0.0048	−2.18±1.30	[41, 42]
125.0	σ_{tot}	0.019	1.08±0.86	[41, 42]
152.4	σ_{tot}	0.08919	−0.14±0.56	[41, 42]
158.9	σ_{tot}	0.01035	−0.36±1.37	[41, 42]
173.1	σ_{tot}	0.01865	1.04±0.71	[41, 42]
242.7	σ_{tot}	0.0294	−0.61±0.63	[41, 42]
253.9	σ_{tot}	0.08172	−0.16±0.65	[41, 42]
263.9	σ_{tot}	0.0305	−0.01±0.42	[41, 42]
282.4	σ_{tot}	0.01629	0.41±1.40	[41, 42]

thermal neutrons using the (n,α) and (n,p) reactions, respectively. Nevertheless, the result for ^{6}Li bears a relation to the problem of the f_π and h_ρ constants, whereas ^{35}Cl showed for the first time a PV effect in the (n,p) channel of neutron capture. The latter was explained by mixing of an s-wave with the known p-wave resonance at the energy E_n=398 eV.

The measurement of the ^{6}Li(n,α)T reaction as described by Andrzejewski *et al.*[45] was performed in the beam of polarized cold neutrons from the VVR-M reaction at the St. Petersburg Institute of Nuclear Physics, Gatchina. The incident beam had an average neutron wavelength of 4.5 A and 80% polarization with intensity $2\cdot10^{10}$ n/sec. The $P_t(\boldsymbol{\sigma}\cdot\mathbf{p}_t)$ P-odd term was measured, where $\mathbf{p}_t$ is the triton momentum. A proportional chamber with 24 sections working in the ionization current mode was used. The target was made of ^{6}LiF layers with thickness 400 and 600 μg/cm^2. The triton component of the reaction was measured, the α particle being absorbed by an additional aluminum foil. The result

$$P_t=-(6.44\pm5.50)\cdot10^{-8}$$

represents no effect but sets constraints on f_π (see Sec. 4).

The P-odd $P_p(\boldsymbol{\sigma}\cdot\mathbf{p})$ correlation in the ^{35}Cl$(n,p)^{35}$S reaction was measured by Antonov *et al.*[46] in another beam channel of the Gatchina VVR-M reactor. The intensity of the 90% polarized thermal-neutron beam was 10^7 n/sec. A thin target of $BaCl_2$ (2 μg/cm^2 thickness) was used because of the low energy of the reaction products (E_p=0.62 MeV). The size of the target was 110×7 cm^2, and it was

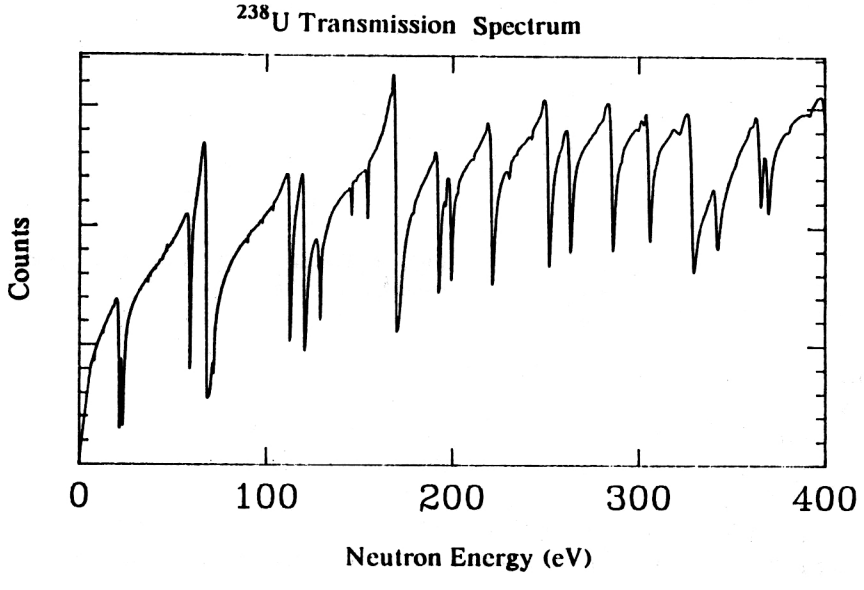

FIG. 3.7. A ^{238}U transmission spectrum up to 400 eV from LANSCE.

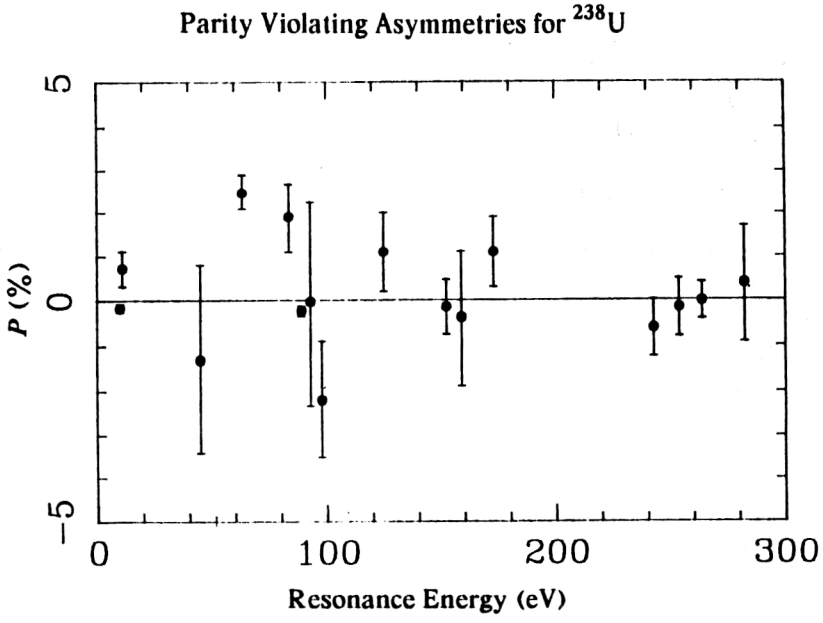

FIG. 3.8. The parity-violating asymmetries for 16 resonances in ^{238}U.

aligned along the beam at a small angle to it. The ionization chamber was set in the proportional regime with an amplification coefficient equal to 50.

The measured effect was $P_p = -(1.51 \pm 0.39) \cdot 10^{-4}$. This is the first observation of parity violation in the (n,p) channel of neutron capture. It was explained as due to PV mixing of the $E_p = 398$ eV and $E_s = -180$ eV resonances. The following value of the weak matrix element was deduced: $M(^{35}\text{Cl}) = (60 \pm 20)$ meV.

4. INTERPRETATION OF THE DATA

4.1. Theoretical models of PV

There are currently two approaches for the explanation of large PV effects in nuclei: the statistical picture of dynamical enhancement and the valence model. According to the first one, the individual matrix elements M of p resonances are random variables, and their variance is identified with M^2. The enhancement is explained by parity admixtures in compound-nucleus states. Calculations of M^2 from the underlying NN interaction have not been performed until very recently. The second approach makes no use of dynamical enhancement and explains PV effects through mixing of single-particle components of the wave function in the entrance channel. It directly relates PV effects to the weak single-particle matrix element, which may be calculated from the weak coupling constants. We shall review both approaches in connection with the experimental data of Sec. 3 as well as the latest theoretical interpretation of the sign-correlation effect in ^{232}Th.

4.1.1. Review of the early literature

The attention of theorists and experimentalists was drawn to the question of PV in nuclear forces by the discovery that weak interactions do not conserve parity.[48–50] Initially it was assumed that the magnitude of parity-violating (PV) effects would be given by the squared ratio of weak-to-strong couplings, which is of order $(G/hr_0^2)^2 \sim 10^{-14}$ (here r_0 is the distance between the nucleons in the nucleus). Gell-Mann and Rosenfeld[51] pointed out that the weak interaction can proceed by emission of one NN^{-1} pair through a strong vertex and absorption through a weak vertex. In this case the relative strength of the PV NN interaction is $\sim 10^{-7}$, as given by Eq. (1). This is the expectation upon which we now base our assumption about the fundamental size of PV in the NN interaction.

In 1959–1960 Haas *et al.*[52] and Blin-Stoyle[53] made controversial estimates of the PV mixing coefficient α [Eq. (3)] and, correspondingly, A_γ for heavy nuclei. Haas *et al.* first suggested that mixing between states of opposite parity would be enhanced in levels near the neutron binding energy by $\sqrt{N}$, where N is the number of contributing excited states of his oscillator shell model near this energy. Expecting $\alpha \sim 10^{-3}$, Haas *et al.* searched for an asymmetry in the γ-ray yield from polarized thermal-neutron capture on ^{113}Cd. No effect was observed, and on this basis they concluded that the amplitude of parity mixing was $\lesssim 4 \cdot 10^{-5}$. Somewhat later, this measurement was repeated by Abov, Krupchitsky, and Oratovsky at the ITEP in Moscow,[1] with the nonzero result $A_\gamma = -(3.7 \pm 0.9) \cdot 10^{-4}$.

This result was explained by Shapiro,[54] who pointed out three possible sources of enhancement: kinematic, structural, and dynamic. The *kinematic* enhancement is the result of interference between electric and magnetic multipoles and gives a factor $R \approx 10$ in Eq. (4). The so-called *structural* enhancement occurs when the parity-allowed transition is suppressed by some singularity in the nuclear structure of the states taking part in the transition. If the same suppression does not apply to the opposite parity component, then there will be an enhancement. The *dynamic* enhancement of Haas *et al.* occurs because the weak matrix element between highly excited levels of opposite parity decreases only as $\sqrt{N}$, while the denominator in Eq. (3) is inversely proportional to the density of states N. Shapiro obtained for d the value $d \approx 10^2$, and therefore the combination of kinematic and dynamic enhancements

can explain the asymmetry $A\sim 10^{-4}$ observed by Abov *et al.*[1]

In 1964 Curtis Michel made an important contribution to the calculation of the weak single-particle potential W in a nucleus. He had obtained an expression which in the current notation is

$$W=\frac{Gg\rho}{m\sqrt{2}}(\boldsymbol{\sigma}\cdot\mathbf{p})=10^{-8}g(\boldsymbol{\sigma}\cdot\mathbf{p}). \tag{22}$$

Here m is the proton mass, ρ is the nucleon density in a nucleus, and g is a renormalization constant taking into account the conditions inside the nucleus. The constant g is expected to be $g\approx 1$, but may be different for protons and neutrons. The coefficient 10^{-8} is valid if $\boldsymbol{\sigma}\cdot\mathbf{p}$ is measured in energy units. Michel had also shown that in this case the amplitude factor F entering the wave function (2) could be estimated as

$$F=g10^{-8}mR. \tag{23}$$

Here R is the radius of a nucleus: $R=r_0A^{1/3}$. Michel[55] and Stodolsky[56] first pointed out the phenomenon of neutron spin rotation due to the weak interaction occurring when a neutron is transmitted through a sample. Based on a single-particle matrix element M_W, their predicted values for the rotation angle were too small to be measurable. Next came the idea of Forte[57] on the role of single-particle p-wave resonances near the neutron threshold, which led to new discoveries. The tail of the absorptive ^{117}Sn resonance at $E_p=1.3$ eV proved to be responsible for the observed neutron spin rotation;[58] however, this was not the ^{124}Sn resonance at $E_p=62$ eV, as was suggested. The corresponding thermal-neutron experiments have been reviewed by Alfimenkov;[5] here we discuss the early literature only to demonstrate their role as a starting point for subsequent models.

4.1.2. s–p compound-level mixing models

Although the idea of dynamic enhancement was often mentioned, and the R-matrix formalism for the description of PV longitudinal effects in (particle, gamma) reactions was known since the paper by Bizzeti,[59] the analysis was not carried through to predict effects in particular neutron p-wave resonances. The models that do so, relying on parity impurities in compound states, are what for brevity we call *s–p mixing* models. An early paper by Karmanov and Lobov[60] pointed out that appreciable enhancement of γ-ray circular polarization might be present near p-wave resonances; the kinematic enhancement was overlooked there.

Sushkov and Flambaum,[61] while explaining the result of the Forte[58] experiment, introduced into the p-resonance wave function the following mixing coefficient:

$$\alpha=\frac{\langle s|V^{\mathrm{PV}}|p\rangle}{E-E_p+i\Gamma_p/2}. \tag{24}$$

Stressing the role of the kinematic factor and using the aforementioned value of the dynamic factor, they estimated the matrix element $M=\langle s|V^{\mathrm{PV}}|p\rangle$ and obtained the value $P\sim 10^{-2}$ for p-wave neutron resonances. Suitable nuclei with low-energy p resonances such as ^{117}Sn, ^{232}Th, and ^{238}U were suggested for study. The kinematic enhancement is due to the fact that the factor $\sqrt{\Gamma_n^s/\Gamma_n^p}$ in Eq. (6) is proportional to $(kR)^{-1}$ due to the angular-momentum barrier penetrability. Later, in Ref. 62, they gave a more elaborate theory of PV effects in neutron resonance reactions. The same problem was successfully addressed by Stodolsky[63,64] in the framework of the K-matrix formalism, resulting in a similar explanation of the enhancement effects near the neutron threshold.

Bunakov and Gudkov[65,66] constructed a theory aimed at correctly describing the energy dependence of PV effects over a broad energy range. They used the framework of the microscopic shell-model approach to nuclear reactions and obtained expressions for the forward–backward asymmetry of scattered neutrons from a longitudinally polarized beam, for the neutron spin rotation angle, and for the longitudinal polarization of unpolarized neutrons transmitted through a sample (the same as P). There are several contributing mechanisms to PV effects in their approach. The leading one, the compound-state mixing, is described by the following formula for the cross-section difference $\Delta\sigma^{\pm}$:

$$\Delta\sigma^{\pm}=\pm 2g_JM\frac{\pi}{k_1^2}(\Gamma_{n0}^s\Gamma_{n0}^p)^{1/2} \times\frac{(E-E_p)\Gamma_s+(E-E_s)\Gamma_p}{[(E-E_p)^2+\Gamma_p^2/4][(E-E_s)^2+\Gamma_s^2/4]}, \tag{25}$$

where parameters of s and p resonances enter quite symmetrically and where neutron reduced widths $\Gamma_{n0}^{s(p)}$ are used along with the neutron wave number k_1 at energy 1 eV. Equation (6) from the Introduction follows from Eq. (25) by calculating P as the ratio of $\Delta\sigma$ to the resonance cross section σ_p near the p-wave resonance energy E_p (with $E-E_s\gg\Gamma_s$).

Bunakov and Gudkov pointed out that in their model the sign of the PV asymmetry P should vary in a random way from resonance to resonance. This happens because the signs of the matrix elements $\langle\phi_s|V^{\mathrm{PV}}|\phi_p\rangle$ and the partial-width amplitudes $(\Gamma_n)^{1/2}$ are random. The sign of the energy denominator will also tend to be random, since the s-wave resonances are present on both sides of the p-wave resonances.

4.1.3. Valence models

The valence model for pure elastic scattering with parity violation was first introduced by Karl and Tadic[67,68] for a spherical potential of constant depth. A significant enhancement of the neutron spin rotation was found, due to the single-particle resonance. The valence theory, taking into account absorptive compound-state resonances, was elaborated by Zaretskiĭ and Sirotkin.[69,70] In the region around a p-wave resonance $[(E-E_s)\gg\Gamma_s]$ the asymmetry was represented as

$$P=2\left[\left[\frac{\Gamma_{ns}(\Gamma_{as}\Gamma_{ap})^{-1/2}}{(E-E_s)}\right.\right.$$

$$+\frac{(E-E_{as})(\Gamma_{as}/\Gamma_{ap})^{1/2}}{(E-E_s)^2+w^2}\Bigg]\frac{FK(\hbar)^2}{mr_0}\Bigg\}$$

$$+2\left\{\frac{(\Gamma_{ns}/\Gamma_{np})^{1/2}}{(E-E_s)}M^{sp}_{\text{stat}}\right\}. \tag{26}$$

Here E_s is the energy of the s-wave resonance, Γ_{ns} and Γ_{np} are the neutron widths of the s and p resonances, respectively, Γ_{as} and Γ_{ap} are the neutron widths of the corresponding single-particle states with positions at E_{as} and E_{ap} (not entering explicitly) in the rectangular potential well, K is the neutron wave number in the well (with $V_0\approx 50$ MeV), m is the neutron mass, $r_0=1.2$ fm is the distance between nucleons, $w\cong 1$ MeV is the spreading width (analogous to the imaginary W term in the optical model), and M^{sp}_{stat} is the statistical matrix element between compound states. The factor that multiplies the two valence terms in brackets is the single-particle valence matrix element M_{val}:

$$\frac{FK(\hbar)^2}{mr_0}\equiv M_{\text{val}}. \tag{27}$$

The relative strength of the weak interaction used by Zaretskiĭ and Sirotkin[69,70] is $F\approx 5\cdot 10^{-7}$. This gives $M_{\text{val}}\approx 25$ eV.

For a given p resonance, the valence contributions from different resonances are correlated: the first term contains Γ_{ns} instead of $\sqrt{\Gamma_{ns}}$ and the same matrix element M_{val} contributes to all p resonances. If the fluctuating statistical term (the third one) overwhelms the first term, the single-particle resonance widths Γ_{ap} and Γ_{as} still give a regular contribution to P through the second term. For example, a constant asymmetry $P\approx 2\cdot 10^{-2}$ is calculated for ^{232}Th at $E=1$ eV. It is predicted that the valence mechanism should dominate for nuclei with low level density (with $D\gg 20$ eV; the light nuclei or the magic ones).

To conduct an analogy with the statistical term one may rearrange the first term in Eq. (26), formally introducing the fluctuating valence matrix element between compound states, M^{sp}_{val}, as

$$M^{sp}_{\text{val}}\equiv\left(\frac{\Gamma_{ns}\Gamma_{np}}{\Gamma_{as}\Gamma_{ap}}\right)^{1/2}M_{\text{val}}. \tag{28}$$

Then the first valence term would have the same shape as the statistical one, and the comparison between them is easier.

The main advantage of this model is the fact that the matrix element is calculable. However, the large value of M_{val} has been scrutinized in other work and was found to be unreasonable from the point of view of the strength of the weak NN interaction. Noguera and Desplanques[71] found that the single-particle weak neutron–nucleus force is too small to account for the PV effects observed in ^{81}Br, ^{111}Cd, ^{117}Sn, and ^{139}La. Flambaum[72,73] calculated M_{val} for ^{232}Th in a square-well potential and found the value $M_{\text{val}}=0.9ig$ (eV) with $g\cong 1$ as the renormalization constant for the weak interaction in nuclei. The constant asymmetry was calculated, and the value $\tilde{P}=1\cdot 10^{-3}g\sqrt{1/E}$ was obtained. Flambaum and Vorov[74] carried out a detailed numerical calculation of the fluctuating matrix element for ^{232}Th in the framework of their valence model with allowance for a nucleon–nucleon residual interaction (Landau–Migdal particle–hole interaction). Their result for the rms value of M^{sp}_{val} is $1.7\cdot 10^{-3}$ meV, making the valence contribution 10^3 times less than the statistical contribution. They used the value of the single-particle matrix element $M_{\text{val}}=0.74$ eV obtained by solving the problem for the Woods–Saxon potential with a spin–orbit interaction.

There is no physical reason for such differences within the framework of one model. To understand the situation we must compare the initial formulas. In Flambaum's work[72] the weak potential is taken in the form

$$W=\varepsilon(\boldsymbol{\sigma}\cdot\mathbf{p}), \tag{29}$$

with the dimensionless constant

$$\varepsilon=\frac{Gg\rho}{m\sqrt{2}}=1.0\cdot 10^{-8}. \tag{30}$$

Zaretskiĭ and Sirotkin[69] chose a different unit of measurement for momentum and spin, so that the potential is taken as

$$W=\frac{F}{mr_0}(\boldsymbol{\sigma}\cdot\mathbf{p}), \tag{31}$$

with $r_0=1.2$ fm and F as a dimensionless constant. Zaretskiĭ and Sirotkin[69,70] use the value $F=5\cdot 10^{-7}$ without entering into the problem of weak NN interactions. However, comparing Eqs. (29) and (31), we obtain the relation

$$F=\varepsilon(r_0/\lambda)=6\varepsilon=6g\cdot 10^{-8}, \tag{32}$$

where λ is the Compton wavelength of the proton, $\lambda=\hbar/mc=0.2$ fm. This is the source of the main difference: the aforesaid F value is equivalent to using a large value $g=10$, which appears unreasonable.

4.2. Matrix elements M_i and rms value of M

Having established that the interaction does contain a small, parity-violating component, it is important to understand the origin of this interaction. The strength of the PV interaction relative to the parity-conserving interaction can be used to assess whether the standard weak interaction can be the source. The matrix elements M_i for p-wave resonances in a compound nucleus are expected to fluctuate randomly. It is necessary to have an ensemble of M_i in order to draw conclusions about the underlying NN interactions in nuclei. The first such data were obtained in the case of resonances in ^{238}U and ^{232}Th. This motivated discussion of the relation of M^2 to the weak-interaction spreading width and to the weak meson coupling constants f_π and h_ρ.

4.2.1. Procedure of obtaining M values

In the statistical theory of the nucleus it is the *distribution* of PV asymmetries and the rms PV matrix element that are of interest. If one knew that the PV asymmetry observed in a given p resonance was due to mixing with a single s resonance, one could use Eq. (6) and values of E_s,

E_p, Γ_s^n, and Γ_p^n to extract the value of the matrix element between the two states. However, in general many s resonances will be mixed into any given p resonance. Then for each p resonance the PV asymmetry is given as a sum over contributions from many s resonances,

$$P_i = \sum_j a_{ij} V_{ij}, \tag{33}$$

where

$$V_{ij} = \langle \phi_{sj} | V^{\mathrm{PV}} | \phi_{pi} \rangle \quad \text{and} \quad a_{ij} = \frac{2}{(E_i - E_j)} \sqrt{\frac{\Gamma_{sj}^n}{\Gamma_{pi}^n}}.$$

The widths and energies of the s-wave resonances are generally known, so that the values of a_{ij} can be calculated. The individual V_{ij} can be considered Gaussian random variables; i.e., they are numbers randomly chosen from a Gaussian distribution that is specified by its mean and variance. In the case of parity violation this distribution should have mean $\langle V_{ij} \rangle = 0$ and variance $\langle V_{ij}^2 \rangle = M^2$. The measured asymmetries are expected to be linear combinations of the Gaussian random variables V_{ij}:

$$\langle P_i \rangle = \sum a_{ij} \langle V_{ij} \rangle = 0 \tag{34}$$

and

$$\langle P_i^2 \rangle = \left\langle \left[\sum_j a_{ij} V_{ij} \right]^2 \right\rangle = \left(\sum_j a_{ij}^2 \right) M^2 = A_i^2 M^2. \tag{35}$$

Therefore, one can estimate M^2 from the ensemble of values of P_i. Of course, the actual variance will be larger because of the experimental uncertainties δ_i:

$$\langle P_i^2 \rangle = [A_i^2 M^2] + \delta_i^2. \tag{36}$$

The procedure used to extract M^2 from the set of values P_i has been detailed by Zhu *et al.*[42] These authors wrote down the probability for measuring a PV asymmetry between P_i and $P_i + \delta P_i$ as

$$F(P_i) dP_i = \frac{1}{[2\pi(M^2 + \delta_{Qi}^2)]^{1/2}} \exp\left(\frac{-Q_i^2}{2(M^2 + \delta_{Qi}^2)} \right) dQ_i, \tag{37}$$

where

$$Q_i = \frac{P_i}{A_i} \quad \text{and} \quad \delta_{Qi} = \frac{\delta_i}{A_i}.$$

Given this probability distribution, one could construct a likelihood function to determine the most probable value of M^2. However, the analysis is complicated by the fact that the spins of the p resonances are not known. For $I_{tgt} = 0$ these can be $j_i = 1/2$ or $3/2$. Only the $j_i = 1/2$ p resonances can exhibit PV due to mixing with $j = 1/2$ s resonances. This problem is solved by taking a statistical approach, assuming that 1/3 of all the observed p resonances have $j = 1/2$, and 2/3 have $j = 3/2$. The distribution of P_i is then a sum of two terms, one for $j = 1/2$ with variance $A_i^2 M^2 + \delta_{Qi}^2$ and another with variance δ_{Qi}^2. The authors of Ref. 41 then construct likelihood functions and extract the most likely value for M^2.

The result for the analysis of 16 p resonances in ^{238}U is $(M^2)^{1/2} = 0.56^{+0.41}_{-0.20}$ meV.[42] For ^{232}Th the same analysis was performed[40] on 23 p resonances, giving $(M^2)^{1/2} = 1.39^{+0.55}_{-0.38}$ meV. These two results are almost within the errors of each other. It is possible to estimate the expected rms value of M, using the dynamical enhancement mechanism. The matrix elements M_i of the compound states are related to the single-particle matrix elements by the relation

$$\sqrt{M^2} = \frac{W}{\sqrt{N}}. \tag{38}$$

Here N is the number of quasiparticle components in the compound nuclear wave function and can be estimated from the relative spacings of compound ($D \sim 10$ eV) and single-particle ($D_0 \sim 1$ MeV) levels: $N \sim 10^5$. Then with $W \sim (0.13\text{–}0.30)$ eV, we obtain the quoted experimental values of M for ^{238}U and ^{232}Th, respectively.

Accurate calculations were made recently by Flambaum[73] with a distinction between the principal and small "nonprincipal" single-particle components of the compound-state wave function (see also Ref. 75, where the essential role of the small components was stressed for the first time). Starting from the weak coupling constants f_π and h_ρ, Flambaum obtained the value $W = 0.9$ eV and, correspondingly, $\sqrt{M^2} \cong 1.0$ meV.

4.2.2. Relation of M^2 to Γ_{spr}^{PV}

French and co-workers have studied[76,77] the effect of a symmetry violation on spectral and strength fluctuations in complicated systems. They describe the transition from symmetry to broken symmetry by mean-square symmetry-violating matrix elements; the M^2 that has been extracted from ^{238}U and ^{232}Th is analogous to the parameter used by French *et al.* The mean-square symmetry-violating (SV) matrix element is quoted in units of the local average level spacing D:

$$\lambda^{\mathrm{SV}} = M^2 / D^2. \tag{39}$$

For the case of violation of time-reversal invariance, French *et al.*[78] have related λ^T to the relative strength α_t of the noninvariant interaction as follows:

$$\lambda^T D = K \alpha_T^2, \tag{40}$$

where K is calculated to vary from $K = 0.7 \cdot 10^5$ eV for ^{169}Er to $K = 2.0 \cdot 10^5$ eV for ^{233}Th and $K = 1.3 \cdot 10^5$ eV for ^{239}U. The spreading width of the symmetry-violating interaction, $\Gamma_{spr}^{\mathrm{SV}}$, is related to $\lambda^{\mathrm{SV}} D$:

$$\Gamma_{spr}^{\mathrm{SV}} \equiv 2\pi \frac{M^2}{D} = \pi \lambda^{\mathrm{SV}} D. \tag{41}$$

One can then quote a spreading width based on the values of M for the ^{238}U and ^{232}Th data of Refs. 42 and 40. For ^{238}U, $\Gamma_{spr}^{\mathrm{PV}} = 0.9^{+1.9}_{-0.5} \cdot 10^{-7}$ eV, and for ^{232}Th, $\Gamma_{spr}^{\mathrm{PV}} = 7.4^{+8.2}_{-3.8} \cdot 10^{-7}$ eV. If one assumes that the relationship in Eq. (40) for time-reversal violation is valid for a PV interaction, then

$$\Gamma_{spr}^{\mathrm{PV}} = 2\pi \alpha_P^2 K. \tag{42}$$

This relation can be used to estimate α_P, the relative strength of the PV interaction, from the value of M^2. The result is that for ^{238}U, $\alpha_P \sim 3 \cdot 10^{-7}$, and for ^{232}Th, $\alpha_P \sim 8 \cdot 10^{-7}$. Given the large error bars on M, the numbers are in agreement.

It is not clear, however, that the numbers K calculated by French *et al.* are applicable to the case of parity violation. The procedure for calculating K involves selection of a set of single-particle basis states. For time-reversal violation, these single-particle levels may be in the same major shell, whereas the PV mixing must involve single-particle levels from different major shells. This will certainly influence the final calculation of K.

4.2.3. Relationship of M^2 to f_π and h_ρ

The relationship of the PV nucleon–nucleon (NN) potential to the weak interaction between quarks has been discussed by Adelberger and Haxton[2] (see also references therein). The weak interaction is described by a phenomenological current–current Lagrangian in terms of charged and neutral weak currents. One component of the PV weak interaction is due to the exchange of $W^\pm$ and Z^0 bosons between nucleons. Because the masses of the W and the Z are large, this exchange will give rise to a short-range interaction. The interaction between nucleons with energies typical of bound nucleons is dominated by the longer-range parts of the interaction. For this reason, the strong NN interaction can be successfully described by a meson-exchange potential. The mesons that must be included are a function of the energy at which the potential is being calculated. At low energies, only the lightest mesons need be included.

The meson-exchange picture can be used to describe the weak NN interaction by using the strong meson–nucleon coupling at one vertex and the weak meson–nucleon coupling at the other. Of course, one could also have the weak coupling acting at both vertices, but this will be about a factor of 10^7 times smaller and can safely be ignored. The number of mesons that can contribute is limited by Barton's theorem if the potential is to conserve TRI and isotopic spin. One can write the PV potential as

$$V^{\mathrm{PV}} = V_\pi + V_{\rho\omega} + V_{2\pi}, \tag{43}$$

where V_π is the potential due to the exchange of charged pions, $V_{\rho\omega}$ is the potential due to the exchange of the vector mesons ρ and ω, and $V_{2\pi}$ is the potential due to the exchange of two pions. The potential $V_{2\pi}$ has been discussed qualitatively, but is generally ignored. The isoscalar interaction has pieces due to both ρ and ω exchange. The pion contributes only to the isovector interaction; ρ and ω can also contribute. The isotensor interaction is only due to ρ exchange. There are therefore six coupling constants required to specify the PNC meson-exchange interaction: f_π, h^0_ρ, h^1_ρ, h^2_ρ, h^0_ω, and h^1_ω. Desplanques, Donoghue, and Holstein[79] have estimated these coupling constants in the Glashow–Weinberg–Salam model. The PV meson-exchange potential therefore allows us to make a connection between the nuclear PV measurements and the underlying quark-model interaction.

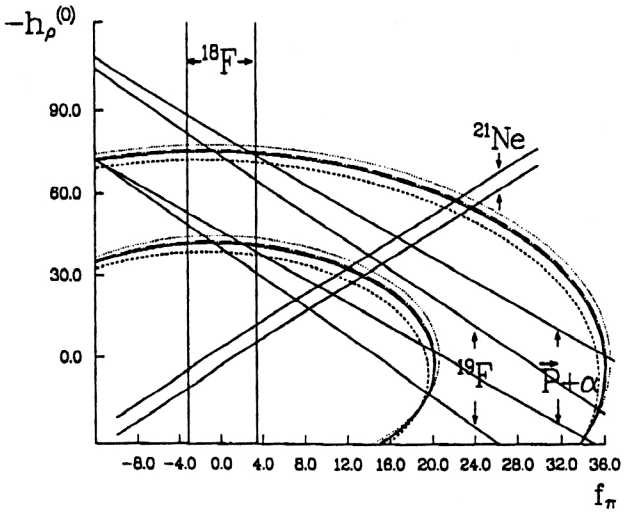

FIG. 4.1. Experimental data on the weak meson–nucleon constants f_π and h^0_ρ; the values are given in units of 10^{-7}.

Johnson, Bowman, and Yoo[80] have developed a theory to relate the mean-square PV matrix element M^2 to the parameters of the PV meson-exchange potential. They first make a connection between M^2 and the PV potential $\alpha_p U_2$ of their model (α_p gives the strength). They find that

$$M^2[\mathrm{keV}^2] = 2.6\alpha_p^2. \tag{44}$$

Essentially the entire PV interaction, as characterized by α_p, is explained by the exchange of π and ρ mesons only. The contributions of the ρ and the π were found to be nearly equal. The value of M^2 was calculated from various theoretical models for the meson coupling constants. All predictions gave a value of M within one standard deviation of the experimental value.[80]

More detail on the sensitivity of the experimental value of M^2 to the coupling constants h^0_ρ and f_π is shown in Fig. 4.1. The curved band shows the limits on f_π and h^0_ρ from the M^2 extracted from the data of Refs. 40 and 42. It was obtained by S. H. Yoo and M. B. Johnson.[81] We can try to understand the appearance of the "neutron curve" in the following way. According to Eq. (34) of Flambaum's paper,[73]

$$M^2 = \frac{\Gamma^1_{spr} D}{\pi} g^2. \tag{45}$$

Here $\Gamma^1_{spr} \cong 0.1$ MeV is the spreading width of the "non-principal" single-particle components, $D = 18$ eV, and the renormalization constant of the weak interaction in the nucleus, g, is a linear function of f_π and h_ρ. Therefore we have the relation

$$M^2 = (af_\pi + bh^0_\rho + c)^2 \tag{46}$$

with known constants a, b, and c which may be obtained from using Ref. 82. Such relations do give the behavior of the curved band in the figure.

We also show the limits from parity-mixing data in the light nuclei ^{19}F, ^{18}F, and ^{21}Ne. Of these, only ^{19}F revealed

a PV effect different from zero. The ^{18}F measurement determines $f_\pi \cong 0$. There is no joint solution for f_π and h_ρ^0 that agrees with all three measurements. It should be pointed out that the ^{21}Ne result is generally regarded as the least certain because of the uncertainty in the nuclear-structure information that is required to extract h_ρ^0 and f_π. There is a solution, $f_\pi \cong 0$ and $h_\rho^0 = -23 \times 10^{-7}$ (in the units of DDH), that satisfies the ^{18}F, ^{19}F, and neutron data.

The width in the neutron-data curve can be reduced with further measurements. This is in contrast to the situation in light nuclei, which has very little prospect for improvement. This initial attempt to relate the neutron measurements of PV in compound resonance states shows promise for obtaining information on the details of the underlying weak *NN* interaction, provided that the uncertainties in the theoretical models and parameters are substantially reduced.

4.2.4. f_π and h_ρ from ^{6}Li(n,α)T

The model of ^{6}Li as a $d+\alpha$ cluster was used by Okunev[47] to extract information on the contributions of charged and neutral currents to the *P*-odd asymmetry in the ^{6}Li reaction. The problem of the weak interaction in the $n+^6$Li system was reduced to a three-body problem with the weak interaction in the *n–d* system.

The following relation between P_t, f_π^1 and h_ρ^0 was obtained:

$$P_t = -(0.45 f_\pi^1 - 0.06 h_\rho^0). \tag{47}$$

With the DDH "best values" of the weak couplings,[79] the expected asymmetry for the reaction is $3 \cdot 10^{-7}$, less than the measured value. With a theoretical value of $h_\rho^0 = -11.4 \cdot 10^{-7}$ and the experimental P_t given in Sec. 3 one obtains

$$f_\pi^1 = -(0.1 \pm 1.2) \cdot 10^{-7}. \tag{48}$$

Provided that the model is correct, this result gives evidence in favor of a small role for the neutral currents in nuclei in accordance with the ^{18}F experiment on γ-quanta circular polarization.

4.3. Sign correlations

One of the significant results of the recent *P*-violation study in neutron resonances is the unexpected finding of a large average value for the *P*-odd asymmetry, averaged over resonances, studied in ^{232}Th. Instead of being random in sign, the longitudinal asymmetry *P* of several resonances is predominantly positive. We know that sign and amplitude correlations appear when a symmetry-violating potential produces mixing of nuclear levels, as in the isospin mixing induced by the Coulomb interaction. Another possible source of correlations is a common doorway state for a group of compound nuclear levels. These possibilities were widely discussed in theoretical studies. However, the origin of the observed phenomenon is not yet understood.

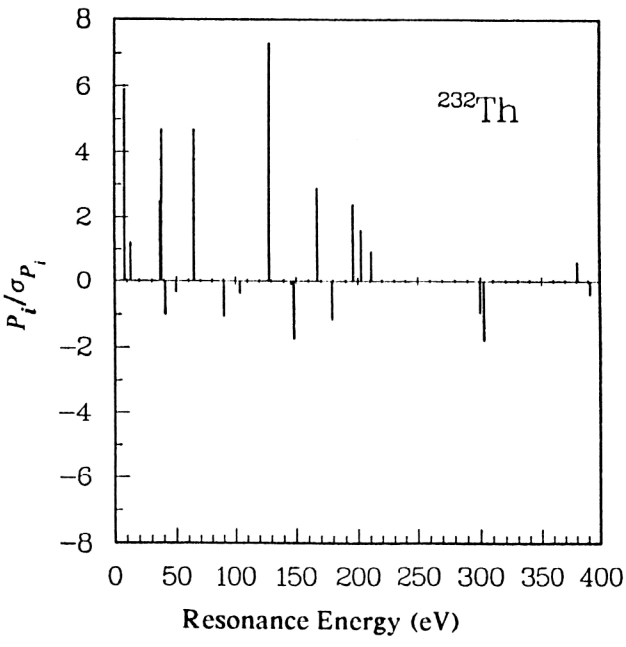

FIG. 4.2. Longitudinal asymmetries of ^{232}Th resonances in units of the experimental uncertainty σ.

4.3.1. Empirical analysis

In Fig. 4.2 the value of the parity-violating asymmetry divided by its uncertainty for ^{232}Th is plotted versus the excitation energy. All seven effects of greater than 2.4σ are positive. This contradicts the expectations of the *sp*-mixing model that the signs of the P_i should be random. The probability of obtaining the same sign for seven out of seven randomly distributed quantities is 1.6%.

An examination of Eq. (33) for P_i shows that a nonrandom sign for the P_i requires a correlation between the signs of: the weak matrix elements M_{ij}, the partial-width amplitudes $\Gamma_{sj}^{1/2}$ and $\Gamma_{pi}^{1/2}$, and the energy denominator $(E_{sj} - E_{pi})$. All these quantities are expected to have randomly distributed signs.

One can see from an analysis of Fig. 4.2 that the data for ^{232}Th could be described by a combination of an asymmetry having the same sign for all resonances and one whose sign and magnitude fluctuate from resonance to resonance. The ^{232}Th data have been analyzed in such a model in Ref. 83. The authors write the PV asymmetry as

$$P_m = -2 \sum \frac{\langle n | V^{\mathrm{PV}} | m \rangle}{E_n - E_m} \sqrt{\frac{\Gamma_n}{\Gamma_m}} + B \sqrt{\frac{1\ \mathrm{eV}}{E}}. \tag{49}$$

The first term describes the fluctuating piece by the *sp*-mixing prediction for *P*. The constant term is given with the energy dependence of the *kinematic* enhancement factor.

In the analysis of Ref. 83 a slightly different assumption is used for the fraction of *p* resonances that have $j = 1/2$ from that used in Ref. 40. The authors use the fact that $p_{1/2}$ resonances are stronger than $p_{3/2}$ resonances to estimate that 44% of the detected *p* resonances have $j = 1/$

2. That analysis yields $M=1.2^{+0.5}_{-0.4}$ meV and $B=8^{+6.2}_{-6.0}\%$. This value of M is slightly smaller than that determined with $B=0$.

4.3.2. Theoretical interpretations

Bowman *et al.*[83] present a possible explanation for the origin of the constant asymmetry. The expression (33) for the parity-violating asymmetry is rewritten to separate the contributions due to the single-particle components of the complicated compound resonances. This *valence* piece corresponds to mixing of s single-particle states that are $1\hbar\omega$ above and below the threshold into the p single-particle state that lies near the threshold. As a result, the energy denominator, partial-width amplitudes, and single-particle matrix element have the same sign for all the p-resonances, thus giving rise to the *constant* asymmetry.

The constant asymmetry is written[83] as

$$\tilde{P}=-2\frac{\gamma_s}{\gamma_p}\sum\frac{\langle G+s|V_{pv}|G+p\rangle}{E_s-E_t}. \tag{50}$$

Here γ_s and γ_p are the single-particle reduced-width amplitudes, and $|G+s\rangle$ and $|G+p\rangle$ are the single-particle configurations. It is estimated theoretically[83] that the value of $|\tilde{P}|$ is $\cong 3\cdot 10^{-2}$. However, a value of $\langle G+s|V_{pv}|G+p\rangle$ of about 50 eV is needed to reproduce the experimental value of B deduced from the ^{232}Th data. This result is inconsistent not only with the size of the single-particle matrix element needed to explain parity mixing in light nuclei, but also with the value $\cong 0.3$ eV determined from the fluctuating asymmetry. Therefore, one must conclude that although this model does introduce a constant asymmetry, with a reasonable single-particle matrix element it is too small to explain the apparent sign correlation in ^{232}Th.

Weidenmüller,[84] Lewenkopf and Weidenmüller,[85] and Gudkov[86] examine all contributions of parity-violating S-matrix elements in some detail. In addition to the internal (compound-state) mixing, there can be parity violation in the formation and in the decay of the compound resonance, as well as direct reaction mixing between the s-wave and p-wave scattering states. The authors of Ref. 85 find that two of the additional terms do contain enhancement factors; they conclude that single-particle matrix elements of order 50 eV are still needed to explain the experimental value of B. In addition, Gudkov argues that the *randomness* in the partial-width amplitudes and in the PNC matrix elements has the same origin: in the compound nuclear wave functions. He demonstrates that the product of two random (but dependent) parameters, each having mean zero, does not necessarily have mean zero. He fails to explain, however, how the energy denominator can have the same sign for all p resonances.

Flambaum[72] presents an argument that the PV effects can be described in terms of the wave functions at the nuclear surface. These are not random because they must all satisfy the same boundary conditions. A doorway-state mechanism through the "quasielastic" part of the compound-state wave function is suggested. In this way a constant sign may emerge.

Koonin *et al.*[87] have performed optical-model calculations indicating that the PV effects produced by *reasonable* PV potentials are 100–1000 times too small to explain the predominance of positive asymmetries measured in ^{232}Th. The shape resonances in the mass dependence of P are predicted with maxima around $A=50$ and $A=150$.

Auerbach and Bowman[88] explained the observed fixed sign and the value of the average asymmetry within the giant $J=0^-$ resonance doorway model, using a large single-particle matrix element $M_W\cong 75$ eV. The size of this matrix element is in contradiction with the value of 2 eV deduced from the experimentally measured PV spreading width using the doorway model.

In summary, many theoretical papers have addressed the question of sign correlations in the parity-violating asymmetries observed in ^{232}Th. Although a number of mechanisms have been identified that could produce the same sign asymmetry in all p resonances, none have been demonstrated to reproduce the magnitude of the constant asymmetry B observed in ^{232}Th.

5. OUTLOOK

Given the difficulty in explaining the apparent sign effect in ^{232}Th, it is extremely important to solidify the experimental evidence. This can be done by improving the statistical accuracy of measurements in ^{232}Th and ^{238}U. Such a study will improve the error bars on the resonances already studied and also allow measurements to be made on weaker p resonances. The chance of accidentally measuring seven positive signs from a distribution with random sign is 1.6%. The probability of a statistical fluctuation is reduced if more significant parity-violating asymmetries can be measured.

The Los Alamos system has been greatly improved since the ^{238}U measurements. In that data set there was only one case of PV greater than 2.4 sigma. With a repeated measurement it should be possible to double or triple the number of significant cases of parity violation. It is extremely important to obtain an improved ^{238}U data set from the point of view of arguments for a constant parity-violating asymmetry.

Thus far, all multiple measurements of parity violation in a single nucleus have been near mass 240. It is important to conduct such measurements near the $3p$ peak of the neutron strength function, about mass 100. This is interesting both from the standpoint of possible sign correlations and for studying the A dependence of the parity-violating spreading width. Such A dependence will be a test of the models of the parity-violating interaction.

We hope that future efforts will prove or disprove the existence of sign correlation in parity-violating asymmetries, measure the weak-interaction matrix elements as a function of the nuclear mass, and continue to look for cases with very large asymmetries as possible candidates for the future study of time-reversal noninvariance.

[1] Yu. G. Abov *et al.*, Phys. Lett. **12**, 25 (1964).
[2] E. G. Adelberger, and W. C. Haxton, Ann. Rev. Nucl. Part. Sci. **35**, 501 (1985).

[3] V. P. Alfimenkov *et al.*, Pis'ma Zh. Eksp. Teor. Fiz. **34**, 308 (1981) [JETP Lett. **34**, 295 (1981)].
[4] V. P. Alfimenkov, S. B. Borzakov, Vo Van Thuan, Yu. D. Mareev, L. B. Pikelner, A. S. Khrykin, and E. I. Sharapov, Nucl. Phys. **A398**, 93 (1983).
[5] V. P. Alfimenkov, Usp. Fiz. Nauk, **144**, 361 (1984) [Sov. Phys. Usp. **27**, 797 (1984)].
[6] P. A. Krupchitsky, *Fundamental Research with Polarized Slow Neutrons* (Springer-Verlag, New York, 1987).
[7] P. Draghicescu, V. I. Lushchikov, V. G. Nikolenko, Yu. V. Taran, and F. L. Shapiro, Phys. Lett. **12**, 334 (1964).
[8] G. A. Keyworth, J. R. Lemley, C. E. Olsen, F. T. Seibel, J. W. T. Dabbs, and N. M. Hill, Phys. Rev. C **8**, 2352 (1973).
[9] Y. Masuda, T. Adachi, S. Ishimoto, E. Kikutani, H. Koiso, and K. Morimoto, Hyperfine Interactions **34**, 143 (1987).
[10] Y. Masuda, S. Ishimoto, M. Ishida, Y. Ishikawa, M. Kohgi, and A. Masaike, Nucl. Instrum. Methods **A264**, 169 (1988).
[11] P. W. Lisowski, C. D. Bowman, G. J. Russell, and S. A. Wender, Nucl. Sci. Eng. **106**, 208 (1990).
[12] J. S. Gilmore, H. A. Robinson, and G. J. Russell, *Advanced Neutron Sources* (Institute of Physics, New York, 1989), p. 455.
[13] A. F. Michaudon and S. A. Wender, LANL Report LA-UR-90-4355, Los Alamos, 1990.
[14] R. J. Macek, in *Proceedings of the 10th Meeting of the International Collaboration on Advanced Neutron Sources*, edited by D. K. Hyer (Los Alamos, 1988).
[15] C. C. Jeffries, *Dynamic Nuclear Orientation* (Wiley, New York, 1963), p. 121.
[16] A. Abragram and M. Borghini, *Progress in Low Temperature Physics*, Vol. 4 (North-Holland, Amsterdam, 1964), p. 384.
[17] J. D. Bowman and W. B. Tippens, private communication, 1990.
[18] V. M. Yuan, C. D. Bowman, J. D. Bowman, J. E. Bush, P. P. J. Delheij, C. M. Frankle, C. R. Gould, D. G. Haase, J. N. Knudson, G. E. Mitchell, S. Penttila, H. Postma, N. R. Roberson, S. J. Seestrom, J. J. Szymanski, B. Tippens, and X. Zhu, Phys. Rev. C **44**, 2187 (1991).
[19] N. R. Roberson *et al.*, Nucl. Instrum. Methods **A326**, 549 (1993).
[20] J. D. Bowman *et al.*, Nucl. Instrum. Methods **A297**, 183 (1990).
[21] J. A. Harvey and N. W. Hill, Nucl. Instrum Methods **162**, 507 (1979).
[22] Y. Masuda, T. Adachi, A. Masaike, and K. Morimoto, Nucl. Phys. **A504**, 269 (1989).
[23] G. F. Knoll, *Radiation Detection and Measurement* (Wiley & Sons, New York, 1989).
[24] B. Efron, SIAM Rev. **21**, 460 (1979).
[25] N. M. Larson, ORNL Report TM-9179/R2, Oak Ridge, 1989.
[26] H. M. Shimizu, Ph.D. Dissertation, Kyoto Univ.; Mem. Fac. Sci. Ser. Phys. **38**, 203 (1992).
[27] C. M. Frankle, J. D. Bowman, J. E. Bush, P. P. J. Delheij, C. R. Gould, D. G. Haase, J. N. Knudson, G. E. Mitchell, S. Penttila, H. Postma, N. R. Roberson, S. J. Seestrom, J. J. Szymanski, V. W. Yuan, and X. Zhu, Phys. Rev. C **46**, 1542 (1992).
[28] H. I. Liou, G. Hacken, F. Rahn, J. Rainwater, M. Slagowitz, and W. Makofske, Phys. Rev. C **10**, 709 (1974).
[29] V. P. Alfimenkov, S. B. Borzakov, Vo Van Thuan, Yu.D. Mareev, L. B. Pikelner, A. S. Khrykin, and E. I. Sharapov, in *Nuclear Data for Science and Technology*, edited by K. H. Bockhoff (1983), p. 773.
[30] V. P. Alfimenkov *et al.*, in *Proceedings of the 6th Soviet Neutron Conf.*, Kiev, 1983, vol. 3, edited by B. D. Kuzminov (Moscow, 1984), p. 408.
[31] V. P. Alfimenkov, Yu.D. Mareev, L. B. Pikelner, V. R. Skoy Skoĭ, and V. N. Shvetsov, Yad. Fiz. **54**, 1489 (1991) [Sov. J. Nucl. Phys. **54**, 907 (1991)].
[32] A. Biryukov *et al.*, Yad. Fiz. **45**, 1511 (1987) [Sov. J. Nucl. Phys. **45**, 937 (1987)].
[33] E. I. Sharapov, S. A. Wender, H. Postma, S. J. Seestrom, C. R. Gould, O. A. Wasson, Yu. P. Popov, and C. D. Bowman, *Capture Gamma-Ray Spectroscopy*, edited by R. W. Hoff (AIP, New York, 1991), p. 756.
[34] C. D. Bowman, J. D. Bowman, and V. W. Yuan, Phys. Rev. C **39**, 1721 (1989).
[35] E. I. Sharapov, in *Proceedings of the Alushta Neutron School*, JINR D3, 4, 17-86-747 (Dubna, 1986), p. 113.
[36] C. M. Frankle *et al.* Phys. Rev. C **45**, 2143 (1992).
[37] D. K. Olsen, ORNL Report TM-8056, Oak Ridge, 1982.
[38] V. P. Alfimenkov *et al.*, JINR Report P3-88-318, Dubna, 1988.
[39] C. M. Frankle, J. D. Bowman, J. E. Bush, P. P. J. Delheij, C. R. Gould, D. G. Haase, J. N. Knudson, G. E. Mitchell, S. Penttila, H. Postma, N. R. Roberson, S. J. Seestrom, J. J. Szymanski, S. H. Yoo, V. W. Yuan, and X. Zhu, Phys. Rev. Lett. **67**, 564 (1991).
[40] C. M. Frankle, J. D. Bowman, J. E. Bush, P. P. J. Delheij, C. R. Gould, D. G. Haase, J. N. Knudson, G. E. Mitchell, S. Penttila, H. Postma, N. R. Roberson, S. J. Seestrom, J. J. Szymanski, V. W. Yuan, X. Zhu, Phys. Rev. C **46**, 778 (1992).
[41] J. D. Bowman, C. D. Bowman, J. E. Bush, P. P. J. Delheij, C. M. Frankle, C. R. Gould, D. G. Haase, J. N. Knudson, G. E. Mitchell, S. Penttila, H. Postma, N. R. Roberson, S. J. Seestrom, J. J. Szymanski, V. W. Yuan, X. Zhu, Phys. Rev. Lett. **65**, 1192 (1990).
[42] X. Zhu, J. D. Bowman, C. D. Bowman, J. E. Bush, P. P. J. Delheij, C. M. Frankle, C. R. Gould, D. G. Haase, J. N. Knudson, G. E. Mitchell, S. Penttila, H. Postma, N. R. Roberson, S. J. Seestrom, J. J. Szymanski, and V. W. Yuan, Phys. Rev. C **46**, 768 (1992).
[43] JENDL-3 Data File for ^{238}U (Japanese Nuclear Data Committee, 1987), evaluation by T. Nakagawa.
[44] ENDF/B-VI Data File for ^{238}U (National Nuclear Data Center, Upton, NY, 1989), evaluation by D. K. Olsen *et al.*
[45] J. Andzejewski, A. D. Antonov, Yu.M. Gledenov, M. P. Mitrikov, Yu.P. Popov, I. S. Okunev, V. G. Peskov, E. V. Shul'gina, and V. A. Vesna, in *Capture Gamma-Ray Spectroscopy*, edited by R. W. Hoff (AIP, New York, 1991), p. 808.
[46] A. D. Antonov, V. A. Vesna, Yu.M. Gledenov, T. S. Zwarova, V. M. Lobashev, I. S. Okunev, Yu.P. Popov, X. Rigol, L. M. Smotrizky, and E. V. Shul'gina, Yad. Fiz. **48**, 305 (1988) [Sov. J. Nucl. Phys. **48**, 193 (1988)].
[47] I. S. Okunev, Thesis, St. Petersburg Institute of Nuclear Physics, Gatchina, 1992.
[48] T. D. Lee and C. N. Yang, Phys. Rev. **104**, 254 (1956).
[49] C. S. Wu *et al.*, Phys. Rev. **105**, 1413 (1957).
[50] R. L. Garwin, L. M. Lederman, and M. Weinreich, Phys. Rev. **105**, 1415 (1957).
[51] M. Gell-Man and A. H. Rosenfeld, Ann. Rev. of Nucl. Sci. **7**, 407 (1957).
[52] R. Haas, L. B. Leopuner, and R. K. Adair, Phys. Rev. **116**, 1221 (1959).
[53] R. J. Blin-Stoyle, Phys. Rev. **105**, 118 (1960), **120**, 181 (1960).
[54] I. S. Shapiro, Usp. Fiz. Nauk. **95**, 647 (1968) [Sov. Phys. Usp. **11**, 582 (1968)].
[55] F. C. Michel, Phys. Rev. **133**, B329 (1964).
[56] L. Stodolsky, Phys. Lett. **50B**, 352 (1974).
[57] M. Forte, in *Fundamental Physics with Reactor Neutrons and Neutrinos*, edited by T. von Egidy (Institute of Physics, 1977).
[58] M. Forte, *et al.*, Phys. Rev. Lett. **45**, 2088 (1980).
[59] P. G. Bizzeti and A. Perego, Phys. Lett. **64B**, 298 (1976).
[60] V. A. Karmanov and G. A. Lobov, Pis'ma Zh. Eksp. Teor. Fiz. **10**, 332 (1969) [JETP Lett. **10**, 212 (1969)].
[61] O. P. Sushkov and V. V. Flaumbaum, Pis'ma Zh. Eksp. Teor. Fiz. **32**, 377 (1980) [JETP Lett. **32**, 352 (1980)] in *Proceedings of the Leningrad Nuclear Physics Institute 16th Winter School* (Leningrad, 1981), p. 200.
[62] V. V. Flambaum and O. P. Sushkov, Nucl. Phys. **412**, 13 (1984).
[63] L. Stodolsky, Phys. Lett. **96B**, 127 (1980).
[64] L. Stodolsky, Nucl. Phys. **197B**, 213 (1982).
[65] V. E. Bunakov and V. P. Gudkov, Z. Phys. A **303**, 285 (1981).
[66] V. E. Bunakov and V. P. Gudkov, Nucl. Phys. **A401**, 93 (1983).
[67] G. Karl and D. Tadic, Phys. Rev. C **16**, 1726 (1977).
[68] G. Karl and D. Tadic, Phys. Rev. C **20**, 1959 (1979).
[69] D. F. Zaretskiĭ and V. I. Sirotkin, Yad. Fiz. **37**, 607 (1983) [Sov. J. Nucl. Phys. **37**, 361 (1983)].
[70] D. F. Zaretskiĭ and V. I. Sirotkin, Yad. Fiz. **42**, 561 (1985) [Sov. J. Nucl. Phys. **42**, 355 (1985)].
[71] S. Noguera and B. Desplanques, Nucl. Phys. **A457**, 189 (1986).
[72] V. V. Flambaum, Phys. Rev. C **45**, 437 (1992).
[73] V. V. Flambaum, in *Proceedings of the 85th Nobel Symposium* (Saltsjiobaden, 1992), to be published.
[74] V. V. Flambaum and O. K. Vorov, Phys. Rev. Lett. (1993, submitted).
[75] S. G. Kadmenskiĭ, V. P. Markushev, and V. I. Furman, Yad. Fiz. **37**, 581 (1983) [Sov. J. Nucl. Phys. **37**, 345 (1983)].
[76] J. B. French, V. K. B. Kota, A. Pandey, and S. Tomsovic, Ann. Phys. (N.Y.) **181**, 198 (1988).
[77] J. B. French, V. K. B. Kota, A. Pandey, and S. Tomsovic, Ann. Phys. (N.Y.) **181**, 235 (1988).
[78] J. B. French, A. Pandey, and J. Smith, in *Tests of Time Reversal Invariance in Neutron Physics*, edited by N. R. Roberson, C. R. Gould,

and J. D. Bowman (World Scientific, Singapore, 1987), p. 80.
[79] B. Desplanques, J. F. Donoghue and B. R. Holstein, Ann. Phys. (N.Y.) **124**, 449 (1980).
[80] M. B. Johnson, J. D. Bowman, and S. H. Yoo, Phys. Rev. Lett. **67**, 310 (1991).
[81] S. H. Yoo, private communication.
[82] V. V. Flambaum, I. B. Khriplovich, and O. P. Sushkov, Phys. Lett. **146B**, p. 367 (1984); INP-Report No. 84–89, Novosibirsk, 1984.
[83] J. D. Bowman, G. T. Garvey, C. R. Gould, A. C. Hayes, and M. B. Johnson, Phys. Rev. Lett., **68**, 780 (1992).
[84] H. A. Weidenmüller, in *Symposium in Honor of K. T. Hecht* (Heidelberg, 1992).
[85] C. H. Lewenkopf and H. A. Weidenmüller, Phys. Rev. C **46**, 2601 (1992).
[86] V. P. Gudkov, Preprint KEK 91-911, Tsukuba, 1991.
[87] S. E. Koonin, C. W. Johnson, and P. Vogel, Phys. Rev. Lett. **69**, 1163 (1992).
[88] N. Auerbach and J. D. Bowman, Phys. Rev. C **46**, 2582 (1992).

This article was published in English in the original Russian journal. It is reproduced here with the stylistic changes by the Translation Editor.